



3 4456 0347639 8

ORNL/TM-11387

# ornl

## OAK RIDGE NATIONAL LABORATORY

**MARTIN MARIETTA**

### Development and Demonstration of Techniques for the Characterization of Reference Coal Structures

L. F. Allard  
E. L. Fuller, Jr.  
T. A. Nolan  
L. A. Harris  
V. J. Tennerly  
D. W. Coffey

OAK RIDGE NATIONAL LABORATORY  
CENTRAL RESEARCH LIBRARY  
CIRCULATION SECTION  
4500N ROOM 175  
**LIBRARY LOAN COPY**  
DO NOT TRANSFER TO ANOTHER PERSON  
If you wish someone else to see this  
report, send in name with report and  
the library will arrange a loan.  
UCN-7969 3 9 77

*Fossil  
Energy  
Program*

OPERATED BY  
MARTIN MARIETTA ENERGY SYSTEMS, INC.  
FOR THE UNITED STATES  
DEPARTMENT OF ENERGY

This report has been reproduced directly from the best available copy.

Available to DOE and DOE contractors from the Office of Scientific and Technical Information, P.O. Box 62, Oak Ridge, TN 37831; prices available from (615) 576-8401, FTS 626-8401.

Available to the public from the National Technical Information Service, U.S. Department of Commerce, 5285 Port Royal Rd., Springfield, VA 22161.

NTIS price codes—Printed Copy: A04 Microfiche A01

This report was prepared as an account of work sponsored by an agency of the United States Government. Neither the United States Government nor any agency thereof, nor any of their employees, makes any warranty, express or implied, or assumes any legal liability or responsibility for the accuracy, completeness, or usefulness of any information, apparatus, product, or process disclosed, or represents that its use would not infringe privately owned rights. Reference herein to any specific commercial product, process, or service by trade name, trademark, manufacturer, or otherwise, does not necessarily constitute or imply its endorsement, recommendation, or favoring by the United States Government or any agency thereof. The views and opinions of authors expressed herein do not necessarily state or reflect those of the United States Government or any agency thereof.

Metals and Ceramics Division

DEVELOPMENT AND DEMONSTRATION OF TECHNIQUES FOR THE  
CHARACTERIZATION OF REFERENCE COAL STRUCTURES

L. F. Allard, E. L. Fuller, Jr., T. A. Nolan,  
L. A. Harris, V. J. Tennery, and D. W. Coffey

Date Published: February 1990

Notice: This document contains information of a  
preliminary nature. It is subject to  
revision or correction and therefore does  
not represent a final report.

Prepared for the  
U.S. DOE Pittsburgh Energy Technology Center  
AA 05 35 00 0

Prepared by the  
OAK RIDGE NATIONAL LABORATORY  
Oak Ridge, Tennessee 37831-6285  
operated by  
MARTIN MARIETTA ENERGY SYSTEMS, INC.  
for the  
U.S. DEPARTMENT OF ENERGY  
under contract DE-AC05-84OR21400



3 4456 0347639 8



## CONTENTS

LIST OF FIGURES . . . . .	iii
ABSTRACT . . . . .	1
1. INTRODUCTION . . . . .	2
1.1 ENVIRONMENTAL INTERACTIONS . . . . .	3
1.2 DIRECT UTILIZATION TECHNOLOGY ISSUES . . . . .	3
1.3 PREMIUM COAL SAMPLE PROGRAM . . . . .	4
2. SCANNING ELECTRON MICROSCOPY AND IMAGE ANALYSES OF COALS . . . . .	6
2.1 INTRODUCTION . . . . .	6
2.2 EXPERIMENTAL TECHNIQUES . . . . .	7
2.2.1 Specimen Preparation . . . . .	7
2.2.2 Microscopy and Image Analyses . . . . .	8
2.3 RESULTS AND DISCUSSION . . . . .	13
3. TRANSMISSION ELECTRON MICROSCOPIC CHARACTERIZATION OF BULK COAL SPECIMENS . . . . .	20
3.1 INTRODUCTION . . . . .	20
3.2 MATERIALS AND METHODS . . . . .	21
3.3 CHARACTERIZATION OF EDS SPECTRAL ARTIFACTS . . . . .	22
4. ELECTRON SPECTROSCOPY FOR CHEMICAL ANALYSIS OF POWDER SURFACES . . . . .	26
4.1 INTRODUCTION . . . . .	26
4.2 EXPERIMENTAL TECHNIQUE . . . . .	26
4.3 RESULTS AND DISCUSSION . . . . .	27
4.3.1 Survey Scan Results . . . . .	27
4.3.2 Nitrogen and Sulfur Measurements . . . . .	27
4.3.3 Survey Scan Results in Range of 0-250 eV . . . . .	28
4.3.4 Types of Carbon . . . . .	31
5. DIFFUSE REFLECTANCE INFRARED SPECTROSCOPY . . . . .	31
5.1 INTRODUCTION . . . . .	31
5.2 EXPERIMENTAL METHOD . . . . .	34
5.3 RESULTS AND DISCUSSION . . . . .	39
5.3.1 Hydrocarbons: Aliphatic and Aromatic . . . . .	40
5.3.2 Aromatic Structures . . . . .	41
5.3.3 Hydroxyls: Phenolic, Alcoholic, Acidic, and Aquatic . . . . .	43
5.3.4 Minerals . . . . .	44

6. CONCLUSIONS . . . . .	44
7. ACKNOWLEDGMENTS . . . . .	45
8. REFERENCES . . . . .	45

## LIST OF FIGURES

Fig. 1.	USDOE Argonne premium coal sample suite: chemical changes in coalification sequence . . . . .	6
Fig. 2.	Scanning electron microscopy images of lignite coal (specimen 801) showing rounded particles covered with many finer particles . . . . .	9
Fig. 3.	Scanning electron microscopy images of bituminous coal (specimen 501) showing particles with angular cleavage surfaces . . . . .	10
Fig. 4.	Scanning electron microscopy images of portions of 200-mesh and 400-mesh nickel grids mounted on a carbon planchet. This specimen is used as a calibration standard for image analysis . . . . .	11
Fig. 5.	Histogram of the Y-feret measurements produced by image analysis shown in Fig. 4 . . . . .	12
Fig. 6.	Histograms of average diameters of particles of lignite (top) and bituminous coal specimens . . . . .	15
Fig. 7.	Histograms of lengths of particles of lignite (top) and bituminous coal specimens . . . . .	16
Fig. 8.	Histograms of perimeters of particles of lignite (top) and bituminous coal specimens . . . . .	17
Fig. 9.	Histograms of aspect ratios of particles of lignite (top) and bituminous coal specimens . . . . .	18
Fig. 10.	Histograms of shape factors of particles of lignite (top) and bituminous coal specimens . . . . .	19
Fig. 11.	Transmission electron micrograph of a section of bituminous coal, normal to the bedding plane (BP horizontal on photo). Point "A" indicates location for spectrum of Fig. 12 . . . . .	24
Fig. 12.	Energy dispersive X-ray spectroscopy spectrum from amorphous region (point "A" in Fig. 11) of bituminous coal. MoK <sub>α</sub> and S/MoL <sub>α</sub> peaks are likely artifacts from specimen preparation, as discussed in text	25

Fig. 13.	Energy dispersive X-ray spectroscopy spectrum from a $\text{Si}_3\text{N}_4$ grain in a $\text{Si}_3\text{N}_4$ thin foil mounted on a Mo ring. The $\text{MoK}_\alpha$ peak, with an intensity equivalent to that obtained from a hole-count test, was observed, but no $\text{MoL}_\alpha$ peak was present. This indicates that Mo was not excited by electrons scattered from the analyses point . . . . .	12
Fig. 14.	Electron spectroscopy for chemical analysis spectrum (0-250 eV) for Illinois #6 coal (A601) . . . . .	29
Fig. 15.	Electron spectroscopy for chemical analysis spectrum (0-250 eV) for Blind Canyon seam coal (A601) . . . . .	29
Fig. 16.	Electron spectroscopy for chemical analysis spectrum (0-250 eV) for Pittsburgh #8 coal (A401) . . . . .	30
Fig. 17.	Electron spectroscopy for chemical analysis spectrum (0-250 eV) for Upper Freeport coal (A101) . . . . .	30
Fig. 18.	Electron spectroscopy for chemical analysis spectrum (0-250 eV) for Pocahontas #3 coal (A501) . . . . .	31
Fig. 19.	Computer-fitted electron spectroscopy for chemical analysis spectrum for carbon C1s photoelectron peaks for Illinois #6 coal (A301) . . . . .	32
Fig. 20.	Computer-fitted electron spectroscopy for chemical analysis spectrum for carbon C1s photoelectron peaks for Blind Canyon coal (A601) . . . . .	32
Fig. 21.	Computer-fitted electron spectroscopy for chemical analysis spectrum for carbon C1s photoelectron peaks for Pittsburgh #8 coal (A401) . . . . .	33
Fig. 22.	Computer-fitted electron spectroscopy for chemical analysis spectrum for carbon C1s photoelectron peaks for Upper Freeport coal (A101) . . . . .	33
Fig. 23.	Computer-fitted electron spectroscopy for chemical analysis spectrum for carbon C1s photoelectron peaks for Pocahontas #3 coal (A501) . . . . .	34
Fig. 24.	Diffuse reflectance infrared spectrum of Upper Freeport coal from Pennsylvania . . . . .	35
Fig. 25.	Diffuse reflectance infrared spectrum of Wyodak coal from Wyoming . . . . .	36
Fig. 26.	Diffuse reflectance infrared spectrum of Illinois #6 coal from Illinois . . . . .	36

Fig. 27. Diffuse reflectance infrared spectrum of Pittsburgh #8 coal from Pennsylvania . . . . .	37
Fig. 28. Diffuse reflectance infrared spectrum of Pocahontas #3 coal from Virginia . . . . .	37
Fig. 29. Diffuse reflectance infrared spectrum of Blind Canyon coal from Utah . . . . .	38
Fig. 30. Diffuse reflectance infrared spectrum of Lewiston-Stockton coal from West Virginia . . . . .	38
Fig. 31. Diffuse reflectance infrared spectrum of Beulah Zap coal from North Dakota . . . . .	39
Fig. 32. Diffuse reflectance infrared spectrum of mixed Argonne premium coal samples . . . . .	40
Fig. 33. Diffuse reflectance infrared spectroscopic evaluation of coalification trends . . . . .	41
Fig. 34. Diffuse reflectance infrared spectroscopic evaluation of rank dependent properties . . . . .	42



DEVELOPMENT AND DEMONSTRATION OF TECHNIQUES FOR THE  
CHARACTERIZATION OF REFERENCE COAL STRUCTURES\*

L. F. Allard, E. L. Fuller, Jr., T. A. Nolan,  
L. A. Harris, V. J. Tennery, and D. W. Coffey

ABSTRACT

Research results on characterizing both the interfaces between coal and associated minerals and the atomic bonding characteristics in coals as a function of coalification are reported. This report includes results from experimental techniques which were explored for providing direct structural and chemical characterization of a number of coals from the Argonne National Laboratory premium coal sample suite. These coals include a range of coal types (ranks) which are of major interest for producing electric power.

Scanning electron microscopy, transmission electron microscopy, electron spectroscopy for chemical analysis, and infrared spectroscopy were applied to a number of coal samples. Specially developed scanning electron microscopy techniques provided insight into the processes occurring when coals are ground to the size required for combustion. The basic fracture mechanisms of the two coals evaluated by this technique varied markedly, showing that each coal rank responds to attrition processes quite differently. Transmission electron microscopy techniques were developed which permitted quantitative elemental analyses to be accomplished in coal samples where the sampling region was no greater than about 10 nm. This instrumental technique has the ability to provide understanding of the structure of very small mineral and other particles within the coal structure.

Electron spectroscopy for chemical analysis measurements were shown to be capable of characterizing the nature of the chemical bonding of various elements on the surface of coal specimens. Results are reported for both the inorganic and organic constituents of ground coal specimens. The various argillic components can be identified and the degree of carbon oxidation can be evaluated for the carbon in coal surfaces. The diffuse reflectance infrared Fourier transformation (DRIFT) technique provided spectroscopy data for coal structures and information on the chemistry and structure of the wide variety of coals in the premium sample suite.

---

\*Research sponsored by the U.S. Department of Energy, Pittsburgh Energy Technology Center, under contract DE-AC05-84OR21400 with Martin Marietta Energy Systems, Inc.

## 1. INTRODUCTION

Combustion of coal has been a primary energy source in the U.S. economy since the beginning of the industrial revolution. More than two decades ago, major legislation was passed regulating the allowable emission of sulfur dioxide, which was recognized as a major pollutant from coal combustion. Since that time, major research efforts have been devoted to methods that minimize sulfur dioxide emissions into the atmosphere. Within the past decade, research has shown that state-of-the-art emission technology still allows potentially serious environmental effects to occur. One example is acidification of lakes and streams, while another is acidification of land masses with detrimental effects on forests. In addition, various nitrogen-bearing oxides produced during combustion processes have received much attention because they contribute to smog formation. Interest has also developed in the environmental effects of various metallic element-bearing emissions from combustion processes, including traces of arsenic, selenium, etc.

These growing concerns about the environmental effects of sulfur dioxide, nitrogen oxide, and metal emissions from coal combustion have resulted in major research efforts within the Office of Fossil Energy of the Department of Energy. A major objective of these efforts is to develop processes to remove most of the contaminants from coal before combustion. The major objective of the research reported herein is to obtain a fundamental understanding of the microstructure and chemical organization of a wide variety of coals and to form a database for eventual design of very low emission coal processing/combustion plants. These data are intended to support a technology for reducing contaminant-bearing materials in coals to a level much lower than current state-of-the-art methods.

The nature of the interfaces between the contaminant element-bearing minerals and the remainder of the coal structure must be characterized to effectively remove these minerals from the coal. Some contaminant elements, such as some of the sulfur, are chemically bound with the carbon in the coal. This particular type of impurity generally has to be removed by special pre-combustion chemical processes. Other impurities, such as

sulfur contained within pyrite or marcasite, can be removed by mechanical/chemical processes, such as grinding followed by flotation, etc.

The research described in this report is currently concentrating on instrumental techniques for characterizing the nature of these interfaces in a number of coals ranging from lignites to anthracites. Special attention is given to microscopic and spectroscopic techniques capable of determining the nature and structure of the sulfur and other mineral type species. These techniques include scanning electron and transmission electron microscopy (SEM and TEM), electron spectroscopy for chemical analysis (ESCA), energy dispersive X-ray spectroscopy (EDS), and DRIFT spectroscopy. A survey made at the start of this research indicated that these techniques could provide the information needed to develop new methods for processing coal to minimize atmospheric contamination with sulfur-bearing gases during combustion. The first coal types being investigated were selected from the Argonne National Laboratory premium coal suite, and will be referred to as "ANL coals" in this report.

### 1.1 ENVIRONMENTAL INTERACTIONS

There is now a consensus in the scientific and governmental communities in the United States that certain chemical species are harmful to the environment when discharged in gaseous form. These chemical species include selected compounds of sulfur and nitrogen. Current combustion technology requires that stringent procedures be used to decrease the precursor nitrogen, sulfur, mineral, and related components in the coal prior to combustion, in order to decrease undesirable effluents from power-generating facilities. More effective processing of coals to remove larger fractions of the minerals contributing to undesirable effluents requires an increased understanding of the structure and chemistry of the coals used in direct combustion processes.

### 1.2 DIRECT UTILIZATION TECHNOLOGY ISSUES

The combustion of coal also produces ash, which creates both environmental and technical/economic problems. Environmental concerns have been raised relative to possible leaching of undesirable metallic elements from ash exposed to natural water drainage systems. Coal ash also generates

costs associated with its removal from the combustor, handling, and storage. Coal ash tends to form deposits on combustor/steam generator walls that can drastically reduce heat transfer to steam generator tubes, thereby decreasing the energy conversion efficiency of power plants and increasing costs. In addition, many of the ash components are corrosive to the structural materials of the combustion system, and thus shorten their life. Finally, the very small fly ash particles that are carried to the stack by the hot combustion gases must also be captured and stored. The processing of fly ash in the combustion gas represents both capital costs and operating costs, which are reflected in higher electrical energy costs, as well as decreases the overall efficiency of the energy production process.

### 1.3 PREMIUM COAL SAMPLE PROGRAM

The U.S. Department of Energy has assigned the Argonne National Laboratory (ANL) responsibility for establishing the Premium Coal Sample Program. This important activity includes acquisition and maintenance of statistically representative samples for a number of coals spanning the range from bituminous to lignite.<sup>1</sup> ANL is also responsible for distributing representative samples of these coals to researchers throughout the United States. Due to the natural instability of many coals after removal from their natural environment, the ANL coals are especially protected from environmental degradation and provide uniform specimens for research purposes. Each ANL coal was acquired from a freshly exposed mine face, stored in an inert atmosphere (nitrogen gas), ground and sieved in an inert atmosphere, and hermetically sealed in brown glass ampoules to avoid exposure to atmospheric reactants and ultraviolet radiation. Considerable effort was expended to assure that these samples represented a cross section of the coal reserves of the United States and represented the major sources of coal feedstocks for the foreseeable future. These sample choices also cover the major portion of the coalification process, excluding peat and anthracite on the extremes.

The general chemical variations and classical ranking of the coals from major U.S. seams are presented in Table 1. The analyses are initial results in an ongoing study<sup>2</sup> of the chemistry and structure of each of

Table 1. Composition of ANL coals

Specimen designation	Coal seam	Description	Composition (wt %)				
			C	H	O	S	Ash <sup>a</sup>
A101	Upper Freeport (PA)	Medium volatile bituminous	87	5.5	4	2.8	13
A202	Wyodak-Anderson (WY)	Subbituminous	74	5.1	19	0.5	8
A301	Illinois #6 (IL)	High volatile bituminous	77	5.7	10	0.5	16
A401	Pittsburgh #8 (PA)	High volatile bituminous	83	5.8	8	1.6	9
A501	Pocahontas #3 (VA)	Low volatile bituminous	91	4.7	3	0.9	5
A601	Blind Canyon (UT)	High volatile bituminous	79	6.0	11	0.5	5
A701	Lewiston-Stockton (WV)	High volatile bituminous	81	5.5	11	0.6	20
A801	Beulah Zap (ND)	Lignite	73	5.3	21	0.8	6

<sup>a</sup>Ash reported as wt % (dry basis).

these materials. This set of preliminary and important data displays the variation of the chemical composition within the classical ranking system, which was developed earlier on the basis of quality of coals (energy content, volatile content, moisture content, etc.). The graphical presentation of the data in Fig. 1 allows visualization of the changes that occur as the coalification process proceeds toward pure carbon. This process is thought to be the source of naturally occurring graphite lodes. The process predominately involves loss of oxygen with a retention of the approximately constant 5.45% of hydrogen, which was present in the original carbohydrate (cellulosic) plant material. Note that the oxygen to carbon ratio decreases over this range of compositions. There also appears to be an inverse relationship between the oxygen and sulfur levels in some coals, for example, the bituminous state represented by Illinois #6 coal at the 77% carbon value.

The sulfur plus oxygen total describes a smooth monotonic trend, which is well within the experimental error and reproducibility of samples

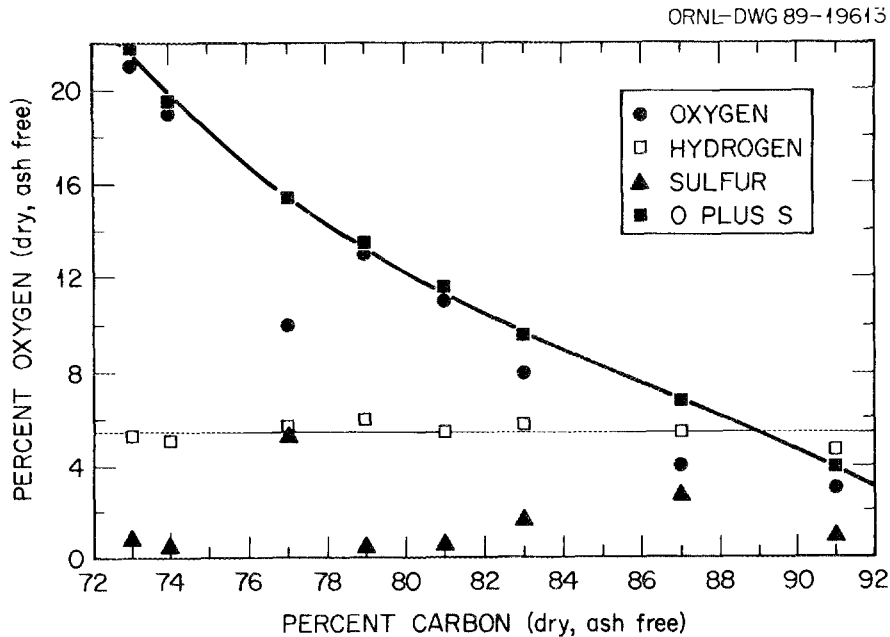


Fig. 1. USDOE Argonne premium coal sample suite: chemical changes in coalification sequence.

of a given coal seam. On the other hand, because the analytical techniques are generally not available for determining the oxygen concentration with high accuracy, the oxygen concentration is normally calculated from a mass balance of the other constituents.

## 2. SCANNING ELECTRON MICROSCOPY AND IMAGE ANALYSES OF COALS

### 2.1 INTRODUCTION

A principal use of the SEM is determination of the surface morphology of materials. An instrument equipped with a proper detector is also capable of determining elemental compositions down to and including boron. When utilized to characterize ground coals, morphological features such as particle size, particle shape, and surface roughness can be directly determined. Computer systems for image analysis remove most of the subjective bias from shape and areal analyses. By analyzing SEM images, characteristics such as aspect ratio and shape factor can be determined and displayed in histograms which allow statistical analyses of a large number of particles.

EDS in the SEM allows elemental analysis of small particles and micro-areas on surfaces of large particles. Because coal is an electrical insulator, the particle surfaces must be made conductive in order to produce adequate images. Rough surfaces on the particles make line-of-sight coating techniques ineffective. A method was developed, therefore, to successfully disperse and coat coal particles. Results of the morphological characterization of two specimens, Lignite A801 and Bituminous A501 (including image analyses), from the ANL coals are presented.

## 2.2 EXPERIMENTAL TECHNIQUES

### 2.2.1 Specimen Preparation

Electrically insulating particles are usually prepared for SEM by first dispersing the powder in a liquid in which the powder is insoluble, typically using ultrasonic agitation. A drop of the resultant suspension is placed upon a planchet. After the liquid has evaporated, the particles and planchet are coated with a thin layer of gold using sputter-coating techniques. This procedure was inadequate for coal particles because electrical charging artifacts in the microscope image were common. The following procedure was developed to overcome the charging phenomenon. The planchet was coated with a thin film of paint that contained electrically conductive colloidal graphite. Coal particles were then dispersed directly onto the wet paint surface. This step resulted in the particles being slightly embedded in and bonded to the paint film. After the paint had dried, excess particles were removed by a stream of freon gas across the planchet surface. The planchet containing the particles was then sputter-coated with gold in a two-step process using a Polaron planar magnetron "cool sputter" coater.<sup>3</sup> The planchet was tilted about 30° from the horizontal in the sputter coater and an approximately 15-nm-thick layer of gold was applied. The specimen was then rotated 180° while maintaining the 30° tilt, and another 15-nm-thick layer of gold was applied. This procedure provided better electrical conductivity at the base of the particles in contact with the substrate. This procedure successfully eliminated most of the electrical charging problems in the SEM. Because a 30-nm-thick layer of gold will likely obscure the finest

detail on particle surfaces, we are developing other coating procedures for ultra-high resolution scanning microscopy of coal particle surfaces.

### 2.2.2 Microscopy and Image Analyses

Microscopy analyses of coal particles were performed using a Hitachi S-800 field emission source SEM with low voltage capability. A Kevex Quantum X-ray detector with light element capability and a Tracor 5500 analyzer provided energy dispersive X-ray elemental analysis. Images were digitally recorded and analyzed using a Tracor 5700 image analysis system.

Considerable effort was required to develop microscopy and image analysis procedures to obtain reliable quantitative results. A requirement for image analysis of particles is that the particles (or at least the particle edges) have sufficient intensity or brightness contrast with the substrate. Brightness difference can be controlled by the microscope accelerating voltage. In this research, accelerating voltages between 2.0 and 20.0 kV were investigated, with the best intensity contrast obtained at 20 kV. All micrographs in this report, therefore, were produced at a 20 kV accelerating voltage.

Figures 2 and 3 show typical SEM images of two samples, Lignite A801 and Bituminous A501, respectively. The uniformity of contrast and other image characteristics indicate that the specimen surfaces had adequate electrical conductivity. Nevertheless, the micrographs reveal regions in some particles that have equal or less intensity than regions of the substrates. Additionally, many particles are in contact with neighbors. The objective of these technique studies was to identify methods for automating coal particle analyses for study in the SEM. The problems noted earlier, and other factors, greatly increase the difficulty of performing automated measurements of coal particle parameters such as particle size and perimeter.

A typical population of specimens requires a series of image processing steps to be performed prior to actual feature analysis to optimize results and to insure statistically significant measurements. Such a sequence of steps was developed for analysis of the coal specimens reported here. The first step that applies to any image processing activity is to determine system performance and calibration with a suitable standard specimen. A standard was created for this coal research

YP9550

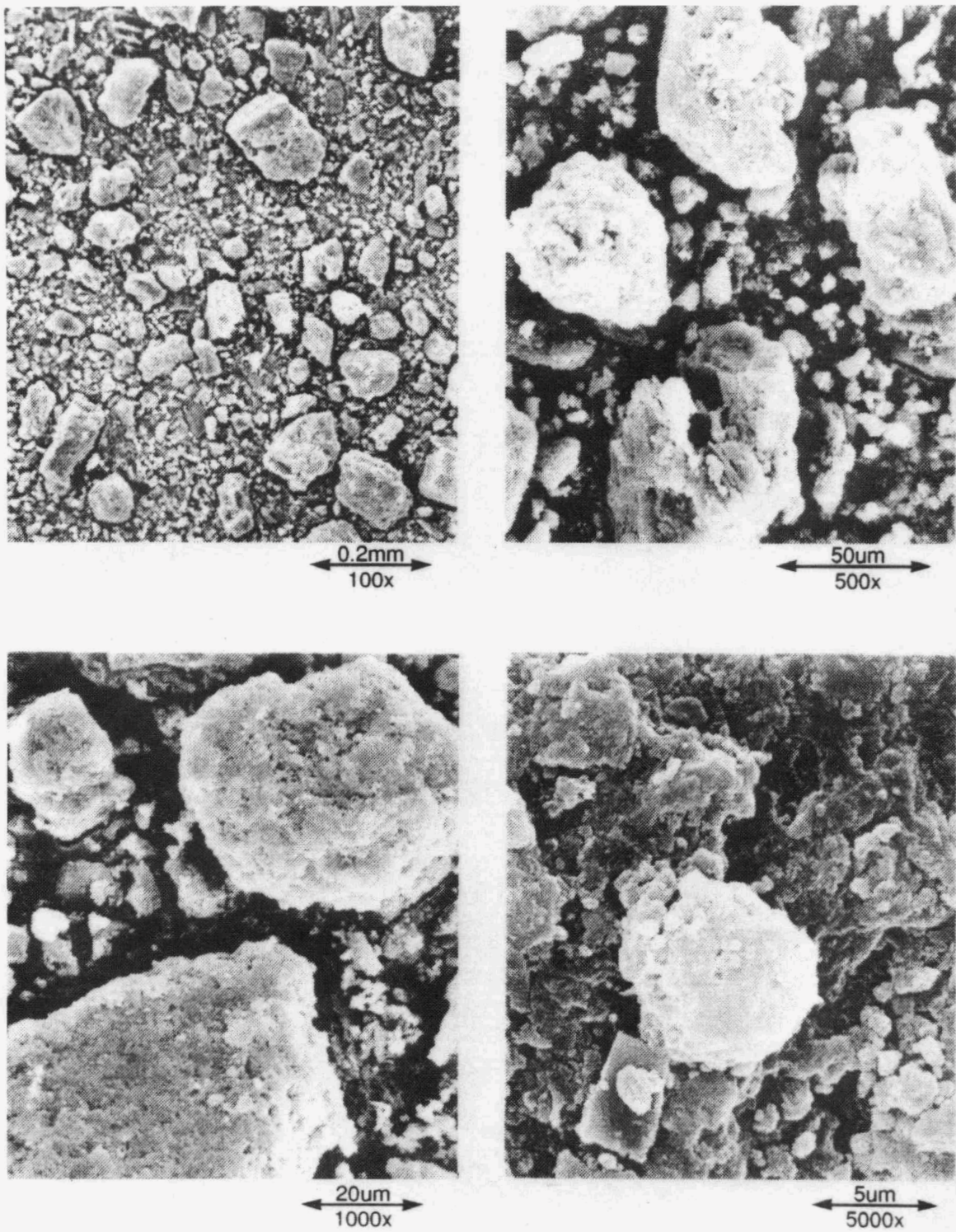
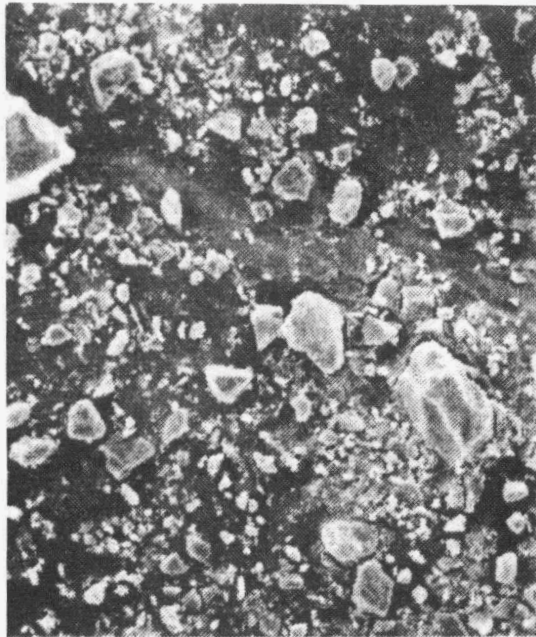
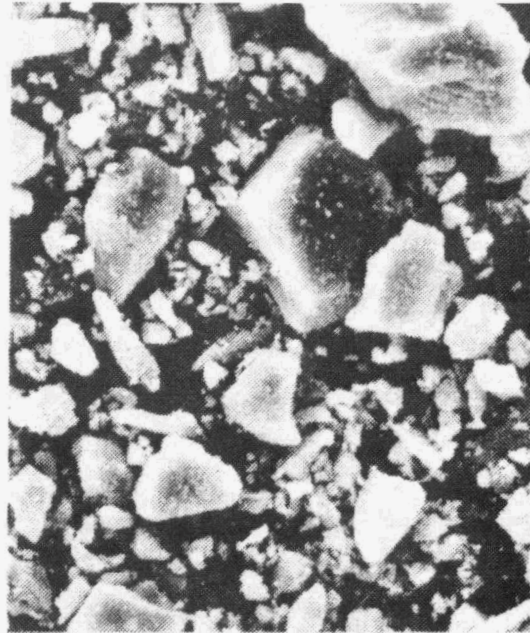


Fig. 2. Scanning electron microscopy images of lignite coal (specimen 801) showing rounded particles covered with many finer particles.

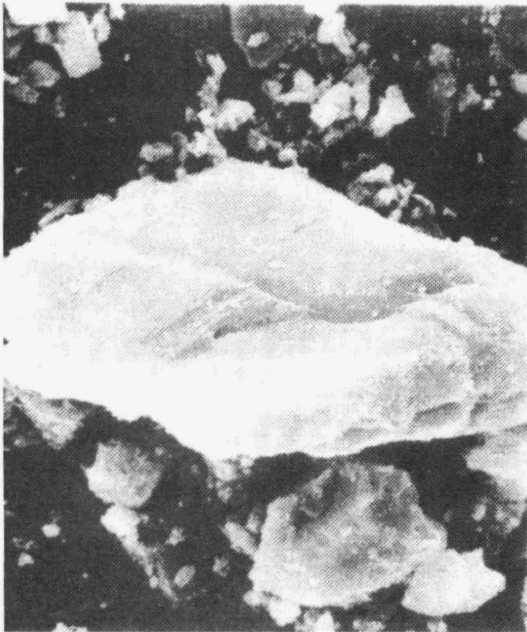
YP9551



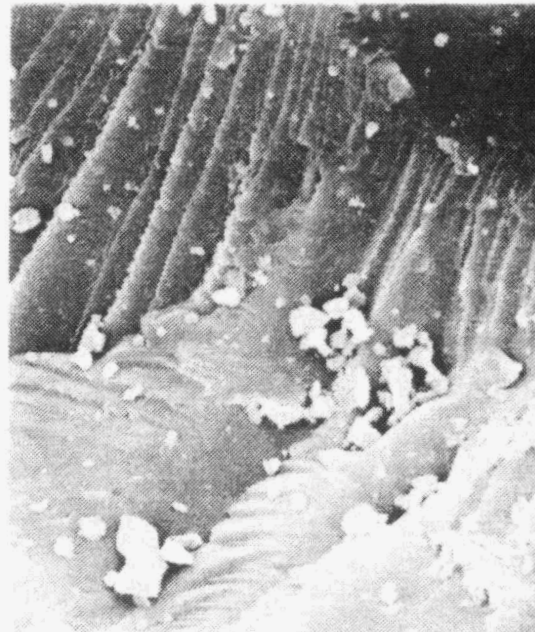
0.2mm  
100x



50um  
500x



20um  
1000x



3um  
3000x

Fig. 3. Scanning electron microscopy images of bituminous coal (specimen 501) showing particles with angular cleavage surfaces.

and was used to confirm the consistency of the SEM-image analysis system. The standard consisted of 200- and 400-mesh samples of nickel screen grid (portions of TEM specimen grids) mounted on a carbon planchet. Figure 4 is a secondary-electron image of this standard showing portions of both screens. The mesh sizes were chosen to fall in the range of sizes of the coal particles; nickel and carbon were chosen to provide large intensity differences. Images of the standard specimen were analyzed using the holes in the screens as the features of interest, and feature size measurements produced by the analysis program were compared to the actual hole dimensions. A typical result of a calibration analysis is shown in Fig. 5 in which the parameter "Y-feret" (a measurement of the width of the holes along the horizontal axis as seen in the micrograph in Fig. 4) is displayed in histogram format. The instrumentation typically produces excellent results with linear errors under 5%.

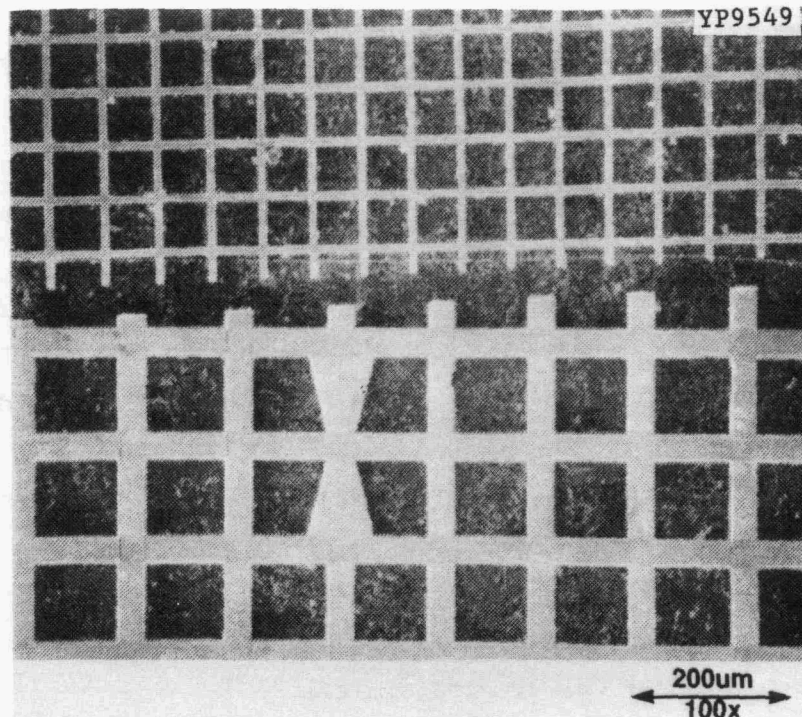


Fig. 4. Scanning electron microscopy images of portions of 200-mesh and 400-mesh nickel grids mounted on a carbon planchet. This specimen is used as a calibration standard for image analysis.

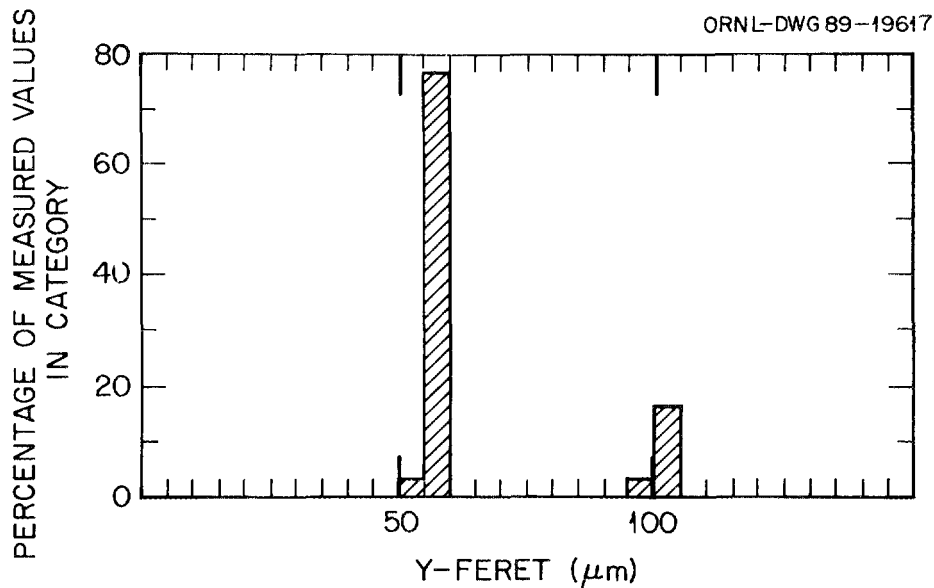


Fig. 5. Histogram of the Y-feret measurements produced by image analysis shown in Fig. 4.

The processing steps needed to optimize actual coal particle images prior to feature analysis are summarized below:

1. Acquire an image of suitable resolution (at least  $512 \times 512$  pixels) and magnification (100X or higher for the coal samples analyzed to date); store image in buffer of analyzer.
2. Digitally expand image grey levels (contrast) to make use of the full range of grey levels in the analyzer (typically 256). Perform median smoothing of the image as required, depending upon residual image noise.
3. Select the band of grey levels that best defines the features to be analyzed and create a binary image of this band.
4. Interactively edit the binary image to facilitate drawing lines and closing features that the analyzer omitted (based on the operator's interpretation of the original image).
5. Accomplish automatic fill-in of all closed features.
6. Interactively use erosion and dilation transforms to effectively separate touching particles.
7. Finally, interactively edit binary images to correct any operator-identified errors in particle separation or joining.

The resultant binary image is then ready for the actual feature analysis followed by the generation of hard copy of the results. As can be seen from the above procedure, considerable operator interaction is required and operator judgment is an important factor.

### 2.3 RESULTS AND DISCUSSION

Procedures have been established for preparation of coal particle specimens that are suitably conductive for measurement of their shape and other characteristics in the SEM. Image analyses using presently available specimen handling procedures have been made as routine as possible. The two coal specimens studied thus far were chosen for their expected considerably different morphologies, which would facilitate procedure development. Although the lignite and bituminous coals are chemically quite different, both ground coal specimens have a very wide range of particle sizes. The problems for image analysis posed by this wide range will be discussed later.

The morphologies of the bituminous coal and lignite coal particles were quite different. The bituminous coal particle surfaces have primarily conchoidal fracture surfaces typical of brittle, glassy, or amorphous materials. The typical glassy fractures are easily visible in the higher magnification views of Fig. 3. The surfaces of larger bituminous coal particles are comprised of several nearly planar brittle fractures which indicates that the particles are angular in nature. This also is true for many smaller particles, although their morphology is more difficult to observe and characterize. The bituminous coal sample also contained very small particles which are particularly evident on the fracture surfaces of larger particles (see the highest magnification view in Fig. 3). The smallest particles in this micrograph are less than 300 nm in diameter.

Both large and small lignite coal particles appear much more rounded than the bituminous coal particles. Their surfaces are porous in appearance and are clearly not simple, exposed brittle fracture surfaces. Occasionally, brittle fracture surfaces were observed for this coal. Also, compared to the bituminous coal sample, fewer of the very small particles were present. These observations are consistent with the

hypothesis that considerable abrasion and agglomeration occurred during the production of this powder. In future work this hypothesis will be confirmed by embedding the powder in a suitable plastic, sectioning and ion-milling, and characterizing the particle surface structures in cross section using a TEM.

Table 2 summarizes measured feature parameters of the samples, while Figs. 6--10 are histograms of selected parameters. The image analysis data are presented primarily to illustrate the techniques that will be used to characterize the suite of coal specimens of interest in this research.

Although many more fields of view of each coal specimen must be analyzed before rigorous statistical conclusions are formed, a few observations were made. Little difference was noted between the two coal samples in parameters related to average diameter and length (see Figs. 6 and 7, respectively). As noted previously, both samples had a very wide range of particle sizes with many very small particles in the bituminous coal specimen. Size information is difficult to extract from a single image magnification on samples with a wide range of sizes. A magnification that allows suitable numbers of the largest particles to be analyzed provides inadequate resolution both in terms of the microscopic image and the image analyzer pixel density for meaningful measurements of the very small particles. Under these circumstances, images at several

Table 2. Image analysis summary for coal particles

Parameter	Lignite A801	Bituminous A501
Area, $\mu\text{m}^2$	1724.46	1376.64
Perimeter, $\mu\text{m}$	166.87	176.36
Shape factor	1.82	2.57
X-feret, $\mu\text{m}$	47.59	46.42
Y-feret, $\mu\text{m}$	44.92	46.79
Average diameter, $\mu\text{m}$	45.41	45.13
Length, $\mu\text{m}$	55.11	55.53
Width, $\mu\text{m}$	36.88	34.67
Aspect ratio	1.59	1.67
Orientation, deg	63.85	66.35

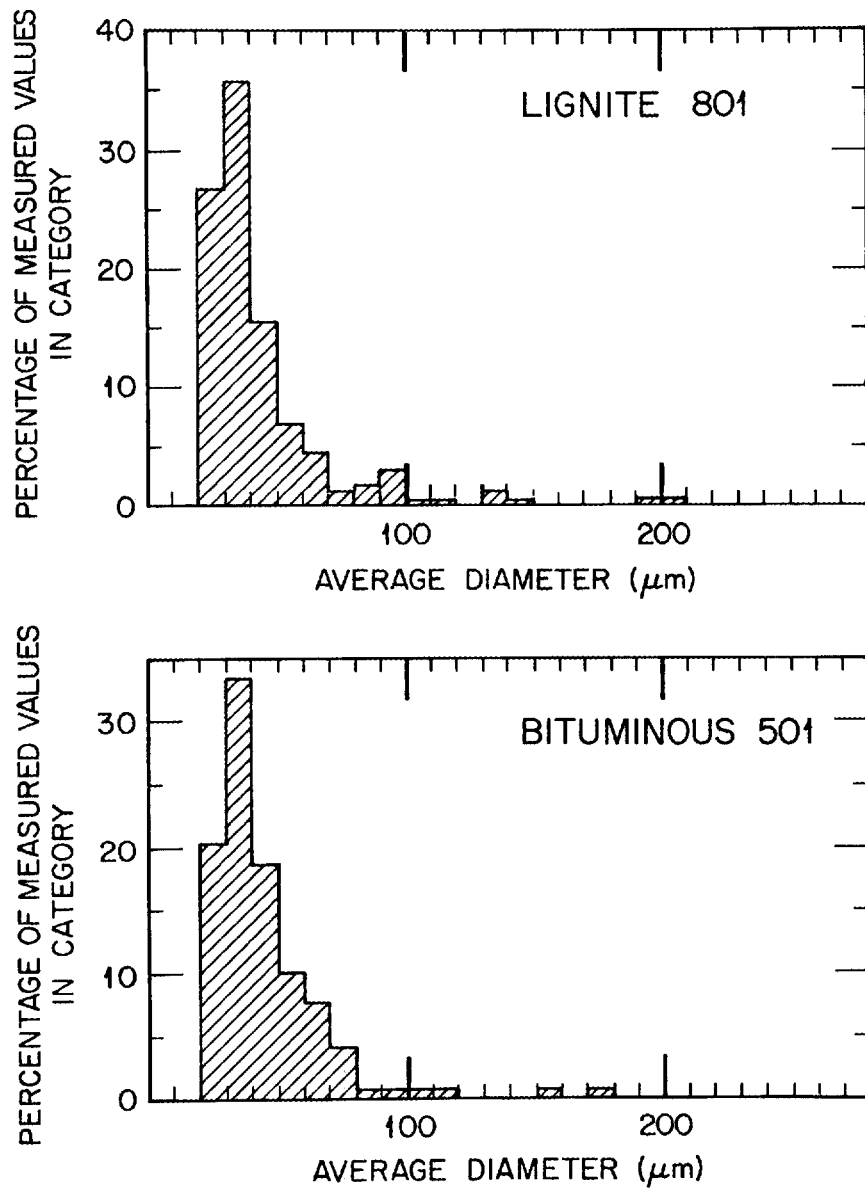


Fig. 6. Histograms of average diameters of particles of lignite (top) and bituminous coal specimens.

ORNL-DWG 89-19619

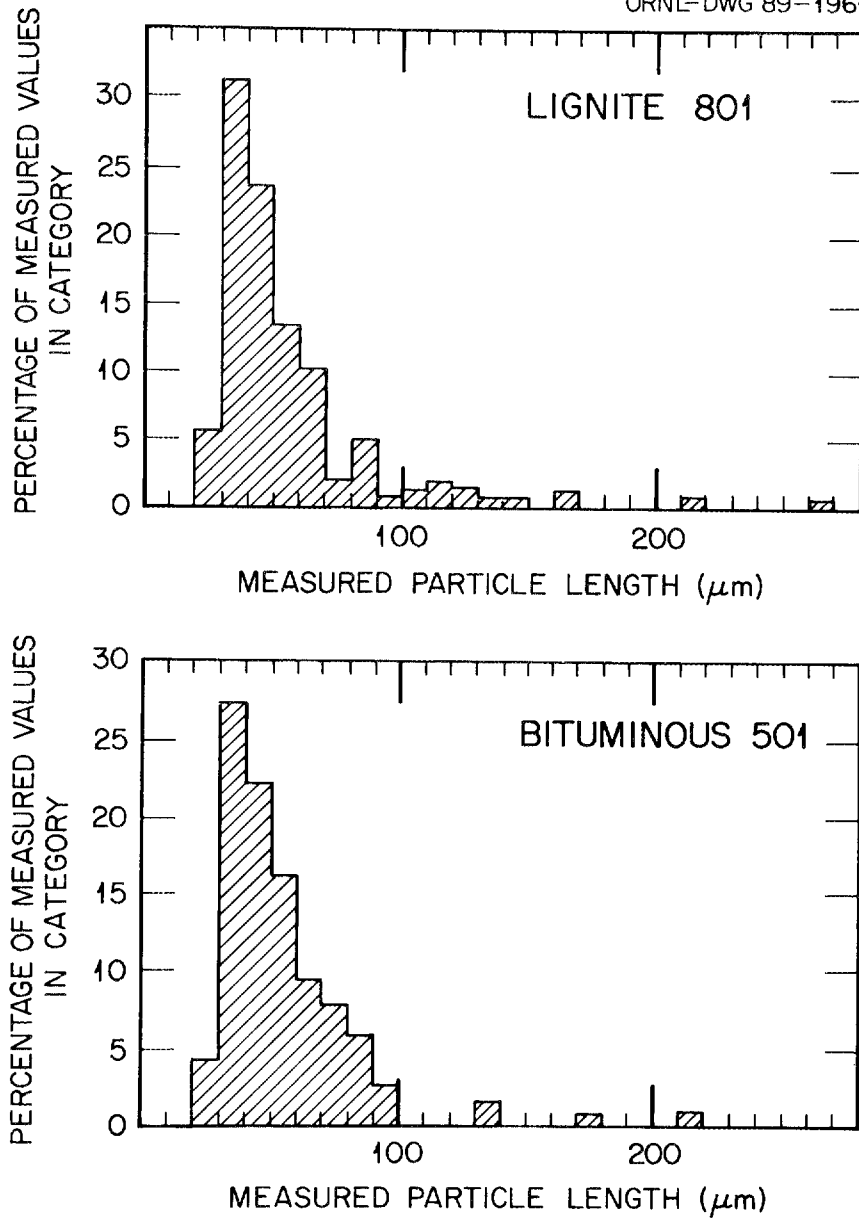


Fig. 7. Histograms of lengths of particles of lignite (top) and bituminous coal specimens.

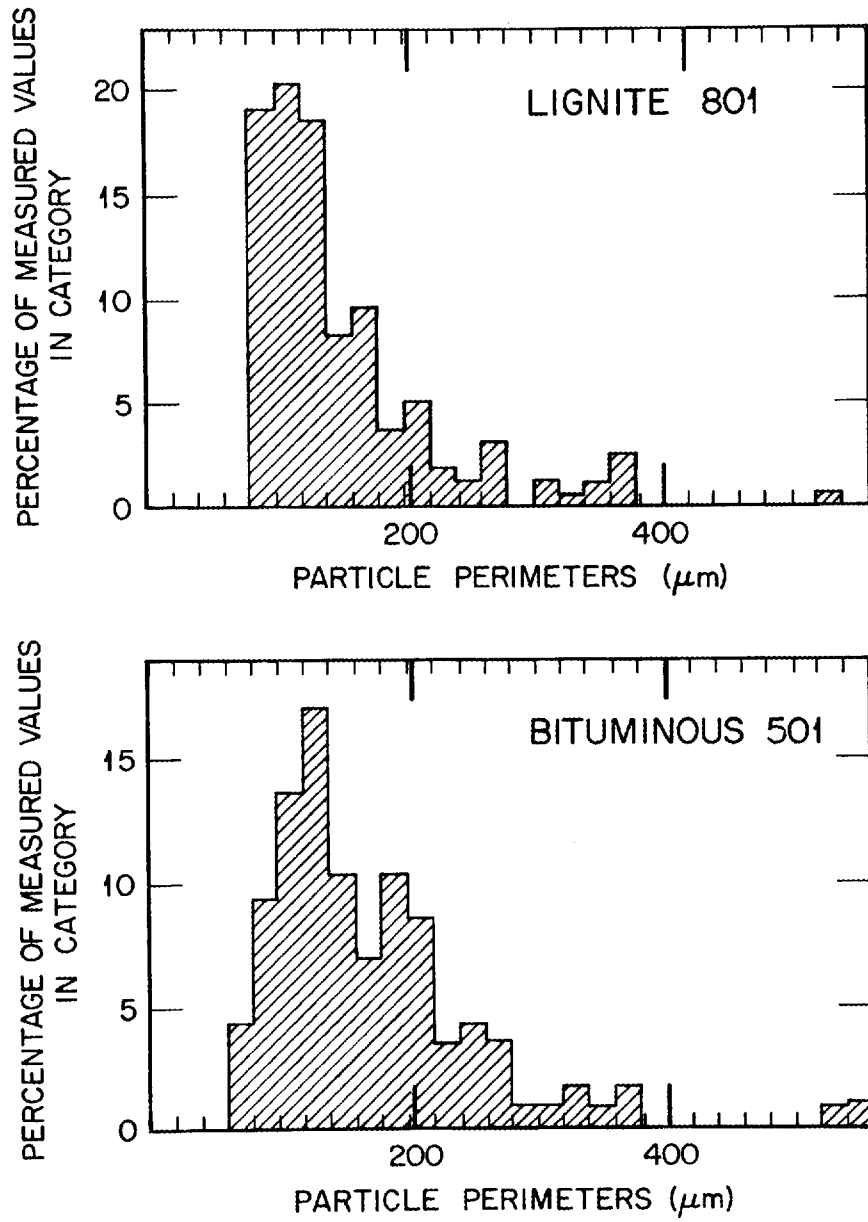


Fig. 8. Histograms of perimeters of particles of lignite (top) and bituminous coal specimens.

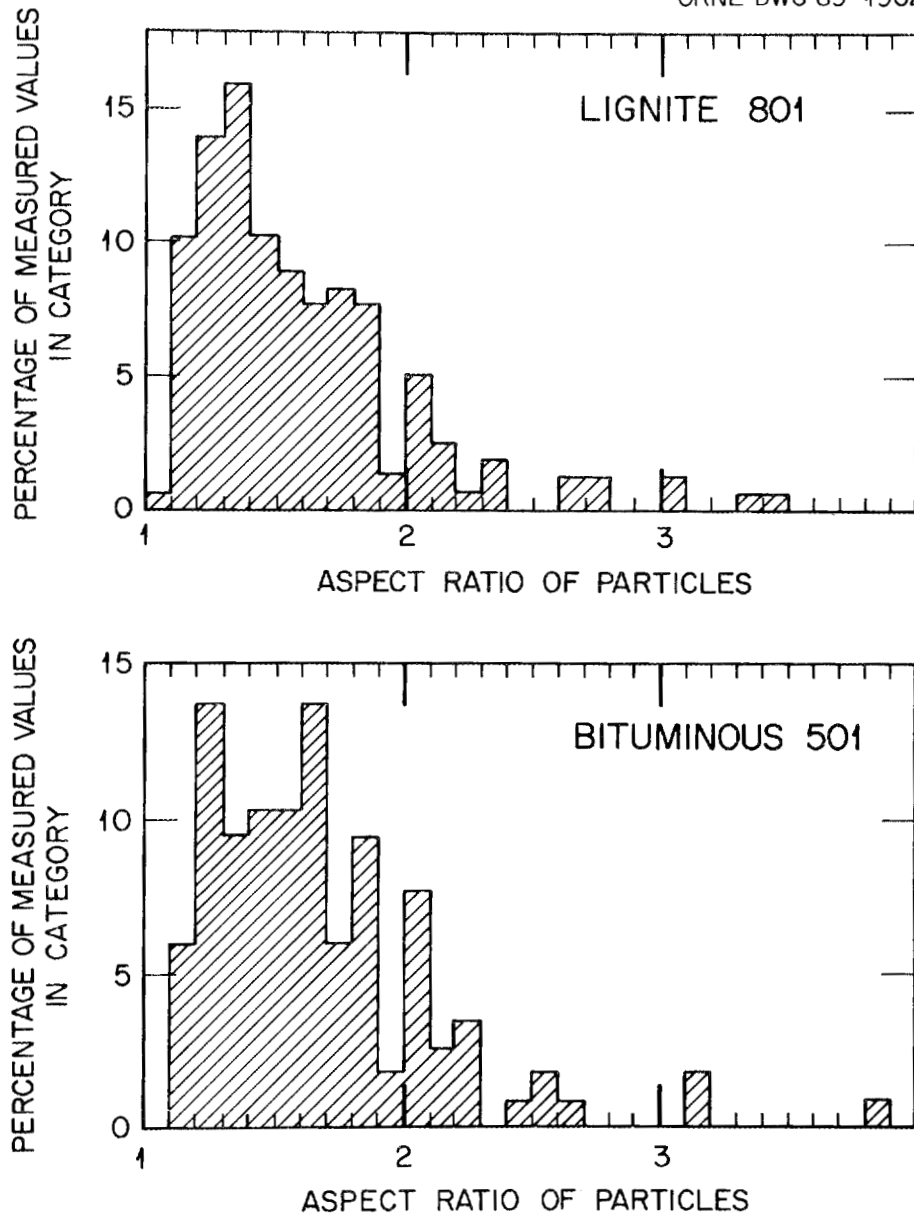


Fig. 9. Histograms of aspect ratios of particles of lignite (top) and bituminous coal specimens.

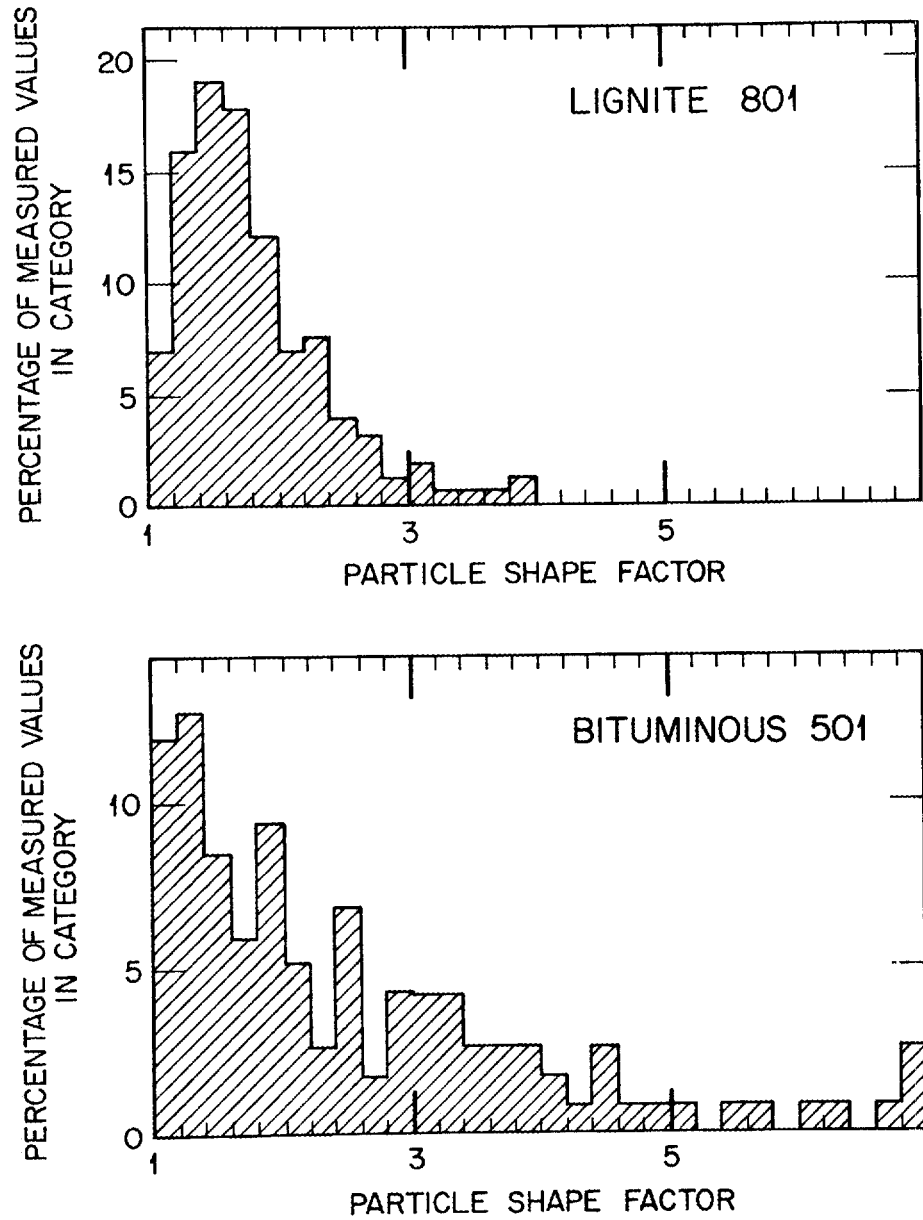


Fig. 10. Histograms of shape factors of particles of lignite (top) and bituminous coal specimens.

magnifications need to be analyzed. The image analyses reported here were all performed on images with an original microscopic magnification of 100X. Since particles less than about 20  $\mu\text{m}$  in diameter were purposefully excluded, the frequency histograms contain no information on the very small particles.

Discernible differences between the two coal samples were observed for parameters more strongly affected by shape (Figs. 8-10). Although there is essentially no difference in particle average diameter or the histogram plots of diameter, there are differences in perimeter, aspect ratio, and shape factor, with the bituminous coal sample having larger values for all three parameters. The histograms also indicate a broader distribution of larger values for the bituminous coal sample. This is the result of the more angular shape of the bituminous coal particles as compared to the rounded lignite coal particles.

Thus far this work has demonstrated that the SEM is a useful tool for characterizing coal particle morphology. In combination with image analysis, particle size and shape differences between coal specimens can be quantified, as demonstrated with two coal specimens from the ANL coals.

### 3. TRANSMISSION ELECTRON MICROSCOPIC CHARACTERIZATION OF BULK COAL SPECIMENS

#### 3.1 INTRODUCTION

The TEM has been used effectively in a number of studies<sup>4</sup> for microstructural characterization of bulk coal specimens at a resolution level far exceeding that possible with conventional optical microscopy. In recent years, the coupling of EDS systems and fine-probe scanning capabilities to the TEM has permitted the characterization of elemental distribution within the microstructure at a spatial resolution at least three orders of magnitude better than that possible with an electron microprobe on bulk specimens. This is a direct result of the nature of the specimen required for measurements with the TEM. The specimen in this case is typically a thin foil on the order of 0.1  $\mu\text{m}$  thick. In such a foil, an incident electron beam with a diameter of about 10 nm will spread only a small amount (due to scattering within the specimen) before exiting the

specimen. Thus, fine particles or other microstructural features in this size range can be analyzed to qualitatively determine the elements present. In many instances, the compositions of phases can be determined quantitatively with relative accuracies of about 3%.

The thin foil specimen that gives such advantages in the TEM for characterizing the structure and chemistry of coal specimens also causes problems which can lead to erroneous results and analyses. In particular, techniques used to prepare thin foils from bulk samples can often introduce artifacts. These artifacts can simulate actual microstructural features and affect the chemistry of the foil. In the present work, bulk coal specimens of different rank and from a variety of locations were characterized by TEM techniques. The initial efforts have been directed both toward developing optimized techniques for thin foil specimen preparation and toward understanding the EDS spectra (and spectral artifacts) so that reliable microstructural and microchemical analyses can be obtained from additional selected specimens.

### 3.2 MATERIALS AND METHODS

Six bulk coal specimens were characterized in the present research. These coals range in rank from lignite to low-volatile bituminous. Thin foil specimens were prepared from slices oriented both parallel and normal to the bedding plane.

Bulk samples of both orientations were attached to a planchet with low melting wax, and sliced to produce 500- $\mu\text{m}$ -thick sections using a low-speed diamond wafering saw. These sections were subsequently mounted and mechanically ground using a precision grinding technique to produce parallel-sided slabs 150  $\mu\text{m}$  thick having one surface finished with 1- $\mu\text{m}$  diamond and the opposing surface finished with 15- $\mu\text{m}$  diamond. Disks, 3 mm in diameter, were core drilled from the ground slabs, and were glued to thin molybdenum rings having a 2-mm-diam central hole. Such supports are necessary to prevent friable specimens from fracturing during the remainder of the preparation process.

These specimens were ground further from the 15- $\mu\text{m}$  finished side using a Gatan, Inc., dimpling machine to produce a dimple having a central thickness of about 30  $\mu\text{m}$  with a 1- $\mu\text{m}$  surface finish. The samples were

ion-milled to perforation using cold-stage techniques on a Gatan Duo-Ion mill, with 6-kV argon ions incident at an angle of 12°. The edges of the holes in such specimens were typically electron-transparent and permitted the microstructure to be imaged appropriately in the TEM.

Thin specimens were examined in a JEOL 2000FX analytical transmission electron microscope (AEM), operated at 200-kV accelerating voltage. EDS spectra were acquired using a Kevex Quantum X-ray detector coupled to a Kevex Delta Class V computer-based analysis system. The Quantum detector is of the ultrathin window type which permits detection of soft X rays characteristic of elements from boron and higher atomic numbers. The detector is especially sensitive to the presence of C, O, and N, elements not detectable on EDS detectors with standard Be windows.

### 3.3 CHARACTERIZATION OF EDS SPECTRAL ARTIFACTS

As the analysis of coal specimens is critically dependent on the ability to unambiguously determine the presence and quantity of sulfur and sulfur-bearing minerals (such as Fe, Cu, and Mn salts) in various microstructural phases, it is important that sources of X rays from these elements (or elements having energy peaks which overlap the peaks of interest) should not be generated as artifacts. In the first stages of the present work, ion-milling techniques that have been successful in the preparation of ceramic specimens were used. Elements present in stage components are not typically deposited on ceramic specimens during the ion-milling process. Unfortunately, the coal specimens often became implanted with both Mo and Cu from the ion-mill stage components and from the Mo support ring, because EDS spectra acquired from the thin specimen exhibited significant peaks from both Cu and Mo. Initial observations of the microstructure of a bituminous coal specimen also showed a nonuniform distribution of fine crystallites which were identified by EDS and electron diffraction techniques to be pure Cu. In a subsequent milling process on the same sample, a different stage with Mo support plates, but no Cu, was used. Milling at a lower accelerating voltage (3 kV) produced a specimen which showed no Cu crystallites in the microstructure and no Cu peaks in the EDS spectrum, indicating that this specimen milling technique was effective, at least for copper, in eliminating the artifacts. A

"hole-count" spectrum, taken with the electron beam positioned within the hole in the specimen, showed a small  $\text{MoK}_\alpha$  peak, but no  $\text{MoL}_\alpha$  peak, which is indicative of excitation of Mo in the specimen support ring by X rays generated in microscope column components above the specimen.

Figure 11 shows a typical microstructure of the bituminous coal specimen normal to the bedding plane. An EDS spectrum (Fig. 12) from an amorphous region of the specimen (labeled "A") in Fig. 11 showed both C and O peaks typical of organic material. It also showed a  $\text{MoK}_\alpha$  peak and a substantial peak at 2.31 keV, which was identified as either a  $\text{MoL}_\alpha$ , a  $\text{SK}_\alpha$  peak, or an overlap of the two. The  $\text{MoL}_\alpha$  peak might have been generated from the Mo support ring by electrons scattered from the specimen area being analyzed. This possibility was tested by obtaining an EDS spectrum under similar operating conditions from a Mo-free specimen of silicon nitride, which was supported by a similar Mo ring. This spectrum (Fig. 13) showed the residual  $\text{MoK}_\alpha$  peak but no  $\text{MoL}_\alpha$  peak, indicating that electron excitation of the Mo ring was not a problem in this instrument. The peak observed at 2.31 keV from the coal specimen, therefore, is either representative of sulfur present in organic material in the specimen, Mo implanted during the thinning process (that was not removed during the modified ion milling), or a combination of both.

The major point here is that standard specimen preparation techniques can generate artifact structures and trace elements, which possibly can lead to erroneous results. In the coal literature, similar specimen preparation techniques have been described, but there was no indication that attention was paid to the possible contamination of the thin specimen by Mo from the ion-milling process. None of the published spectra show peaks higher than 10 keV in energy. This higher energy range is required to determine if the  $\text{MoK}_\alpha$  peak at 17.47 keV is present. Previously published EDS analyses of sulfur in the organic matter in coal specimens might have been affected by the process described above. In future work, tantalum stage components will be used in the ion-milling process to completely eliminate the possibility of contamination of the specimen by Mo. Only with this improvement can sulfur and sulfur-bearing phases be unambiguously analyzed and characterized.



Fig. 11. Transmission electron micrograph of a section of bituminous coal, normal to the bedding plane (BP horizontal on photo). Point "A" indicates location for spectrum of Fig. 12.

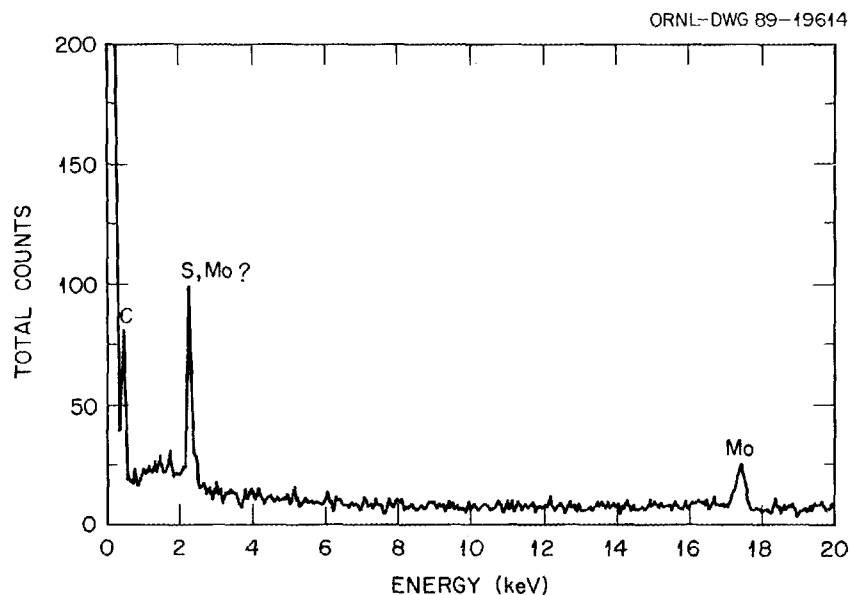


Fig. 12. Energy dispersive X-ray spectroscopy spectrum from amorphous region (point "A" in Fig. 11) of bituminous coal.  $\text{MoK}_\alpha$  and  $\text{S/MoL}_\alpha$  peaks are likely artifacts from specimen preparation, as discussed in text.

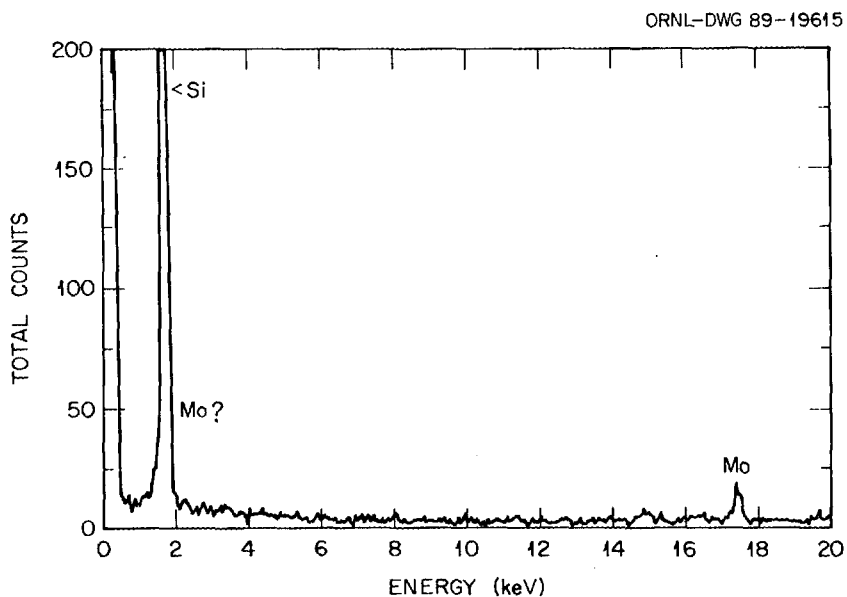


Fig. 13. Energy dispersive X-ray spectroscopy spectrum from a  $\text{Si}_3\text{N}_4$  grain in a  $\text{Si}_3\text{N}_4$  thin foil mounted on a Mo ring. The  $\text{MoK}_\alpha$  peak, with an intensity equivalent to that obtained from a hole-count test, was observed, but no  $\text{MoL}_\alpha$  peak was present. This indicates that Mo was not excited by electrons scattered from the analyses point.

#### 4. ELECTRON SPECTROSCOPY FOR CHEMICAL ANALYSIS OF POWDER SURFACES

##### 4.1 INTRODUCTION

ESCA uses monoenergetic soft X rays to irradiate a sample surface. The X rays excite the atoms on the sample surface by the photoelectric effect, resulting in the emission of photoejected electrons whose kinetic energies are characteristic of the elements in the sample surface. Typically, the mean free path (escape depth) of the photoejected electrons range from 0.5 to 4 nm for metals and ceramics, and from 4.0 to 10 nm for polymers or organic materials such as coal. The sample area analyzed may vary from 150  $\mu\text{m}^2$  to 4 by 10 mm depending upon the specific instrument. Chemical information obtained with ESCA ranges from atomic concentrations of all elements in a sample (except for hydrogen and helium) to information on the chemical states of the elements.

In the past two decades, coal researchers have recognized the potential of ESCA for characterizing coal since the technological utilization of coal is closely tied to its surface properties.<sup>5-7</sup> ESCA studies have shown that the technique differentiates between various chemical states of carbon, including hydrocarbons, carbon-oxygen, and metal-carbon bonds. In addition, the technique can potentially distinguish metal sulfides and nitrides in organic complexes. These capabilities became significant in the present work when we attempted to compare coal chemistry changes as a function of oxidation.

##### 4.2 EXPERIMENTAL TECHNIQUE

Powdered coal samples (~100 mesh) from the ANL coals were studied by ESCA. The coal powders were attached to stainless steel sample stubs by double-sided adhesive tape. No special methods were used to protect the powders from the atmosphere other than storing in sealed jars prior to mounting and installation in the introduction chamber of the ESCA system.

The ESCA measurements were made with a Physical Electronics Model 5100 ESCA system. Spectra were obtained with  $\text{MgK}_\alpha$  radiation (1253.6 eV) using a concentric hemispherical analyzer for analyses of the photoelectron energies. Photoelectron peak positions were corrected for charging by

referencing to the carbon (C1s) peak at a binding energy of 284.6 eV. Survey scans (0-1000 eV) were obtained (pass energy 71.55 eV) for each specimen to identify the elements. Subsequently, narrow scans (20 eV) for each of the identified elements were carried out for extended times with a total multielement analysis of 10 h per coal sample. Relative atomic concentrations of the major and minor elements were computed for each of five samples using peak areas and established elemental sensitivity factors.

#### 4.3 RESULTS AND DISCUSSION

##### 4.3.1 Survey Scan Results

ESCA survey scans for all five samples over the range 0-1000 eV (in binding energy) showed essentially carbon (C1s) and oxygen (O1s) photoelectron peaks. Shorter survey scans over the ranges 0-250, 250-500, 500-750, and 750-1000 eV served to identify the minor and trace elements in the coal samples. Once the identities of all elements were determined, multielement analyses were done for each coal sample. Data obtained in this manner permitted determination of the atomic concentration of elements for the five samples.

A comparison of the atomic concentrations of elements for the five coal samples is presented in Table 3. Large differences were found between sample A301 (Illinois #6, a high-volatile bituminous coal) and the other four coal samples. For example, the carbon content of sample A301 (about 64%) was significantly lower than for the other coal samples, which average about 85%. On the other hand, oxygen in sample A301 is greater than twice the amount found in any of the other coal samples. Additional examination of this table also reveals greater amounts of silicon and aluminum in sample A301 compared to the other four coals. These observations indicate that sample A301 contains much more mineral matter than the other members of this set.

##### 4.3.2 Nitrogen and Sulfur Measurements

Nitrogen is present in all coal samples examined to date. Preliminary analyses of the nitrogen photoelectron peaks in sample A301 suggest two forms of nitrogen; namely, a nitrate (402.0 eV) and an organic compound,

perhaps pyridine (399.2 eV). These data are very preliminary, but it is encouraging that the spectrometer can discriminate these two forms of nitrogen. Similarly, sulfur observed at a peak of 163.6 eV may be of organic origin, because sulfides and sulfates do not explain this particular sulfur energy.

#### 4.3.3 Survey Scan Results in Range of 0-250 eV

Figures 14-18 are survey ESCA spectra obtained over the range 0-250 eV for coal samples A301, A601, A401, A101, and A501, respectively. These spectra serve to illustrate the presence of the typical mineral-forming elements (Si, Al, and Mg) usually observed in coals. Computer-fitted curves for the Si2p and Al2p energies suggest that silicon was present in two different energy states, whereas aluminum was present in only one energy state (compound). These conclusions are based upon the full width half maximum (FWHM) values for these electrons for these two elements, i.e., the FWHM for Si2p is greater than acceptable for a single state. X-ray diffraction data for these samples revealed quartz and kaolinite, which is consistent with observations made with ESCA. The photoelectron line at 240 eV in Figs. 14-18 was caused by MgK $\beta$  interaction with carbon.

Table 3. Atomic concentration of elements in selected coal samples

Elements	Coal samples				
	A301	A601	A401	A101	A501
C	64.08	85.67	86.65	85.36	87.81
O	24.55	10.65	9.70	9.74	8.14
Si	6.02	2.32	1.83	2.92	2.53
Al	2.73	1.37	0.95	0.24	
N	0.60	P <sup>a</sup>	0.88	0.96	0.47
S	P	P	P	P	P
Mg	2.03			0.78	1.05
Na	P				

<sup>a</sup>P = Present.

ORNL-DWG 90-2102

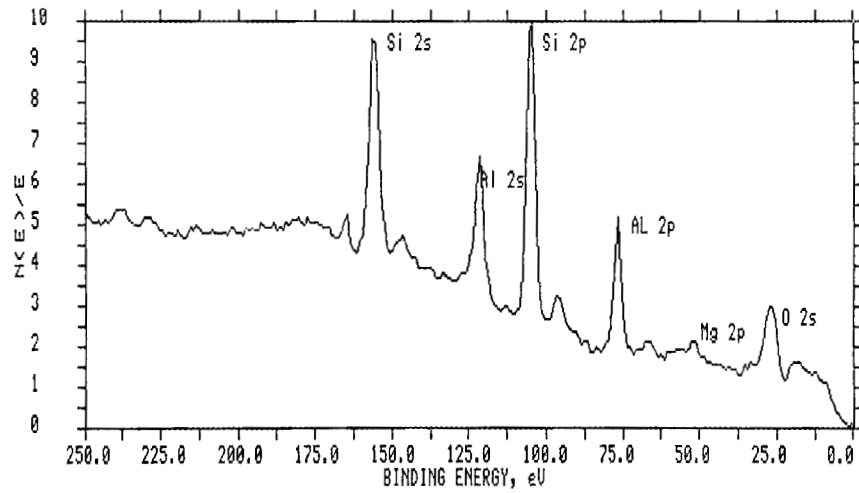


Fig. 14. Electron spectroscopy for chemical analysis spectrum (0-250 eV) for Illinois #6 coal (A601).

ORNL-DWG 90-2103

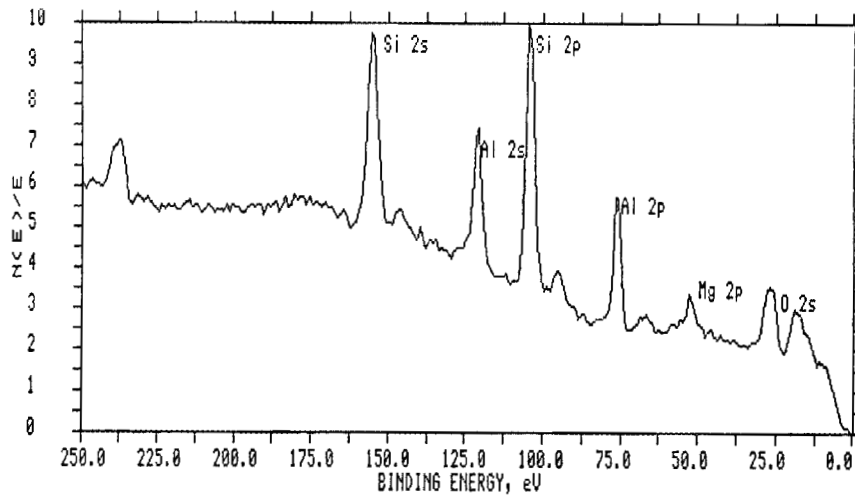


Fig. 15. Electron spectroscopy for chemical analysis spectrum (0-250 eV) for Blind Canyon seam coal (A601).

ORNL-DWG 90-2104

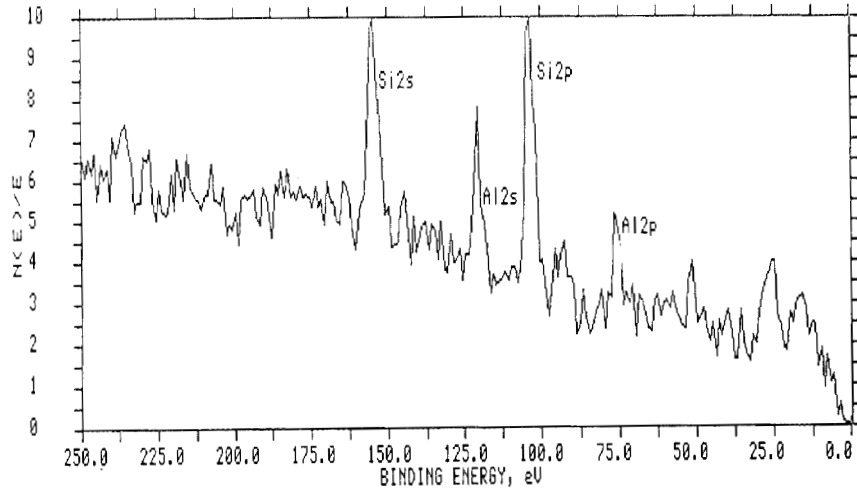


Fig. 16. Electron spectroscopy for chemical analysis spectrum (0-250 eV) for Pittsburgh #8 coal (A401).

ORNL-DWG 90-2105

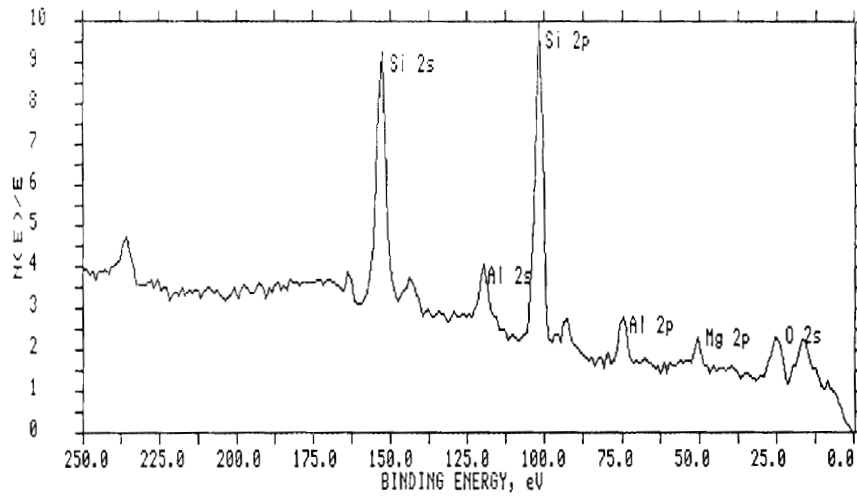


Fig. 17. Electron spectroscopy for chemical analysis spectrum (0-250 eV) for Upper Freeport coal (A101).

ORNL-DWG 90-2106

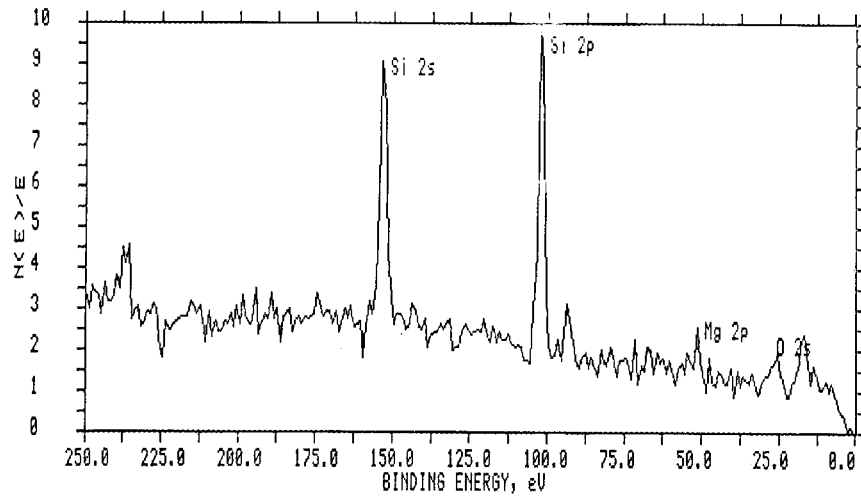


Fig. 18. Electron spectroscopy for chemical analysis spectrum (0-250 eV) for Pocahontas #3 coal (A501).

#### 4.3.4 Types of Carbon

Narrow scan (20 eV) high resolution ESCA spectra for the carbon (C1s) photoelectron peak in the five samples are presented in Figs. 19-23. A skewing of the C1s peak to higher binding energies for all coal samples suggests the presence of carbon/oxygen functional groups. The fit was performed using published data on the relative positions of carbon-oxygen photoelectron lines with respect to the hydrocarbon line (nominally at 284.6 eV). These data are preliminary since improvements in the fit to the line profiles are still possible, i.e., improving the least-squares fit either by placing additional lines within the experimental line envelope or/and modifying selected parameters. Future efforts will be directed at improvements in line profile fit for all elements.

## 5. DIFFUSE REFLECTANCE INFRARED SPECTROSCOPY

### 5.1 INTRODUCTION

Infrared spectroscopic techniques have been very helpful in elucidating the chemistry and structure of coals,<sup>8</sup> and the advent of

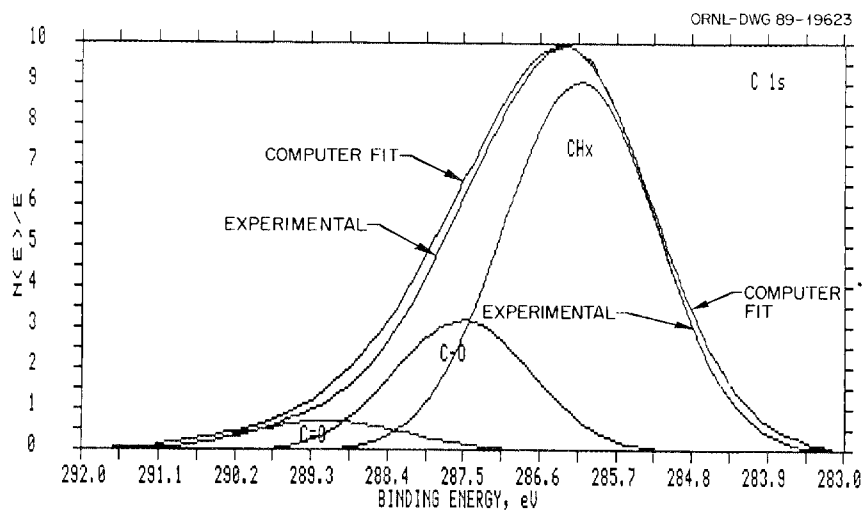


Fig. 19. Computer-fitted electron spectroscopy for chemical analysis spectrum for carbon C1s photoelectron peaks for Illinois #6 coal (A301).

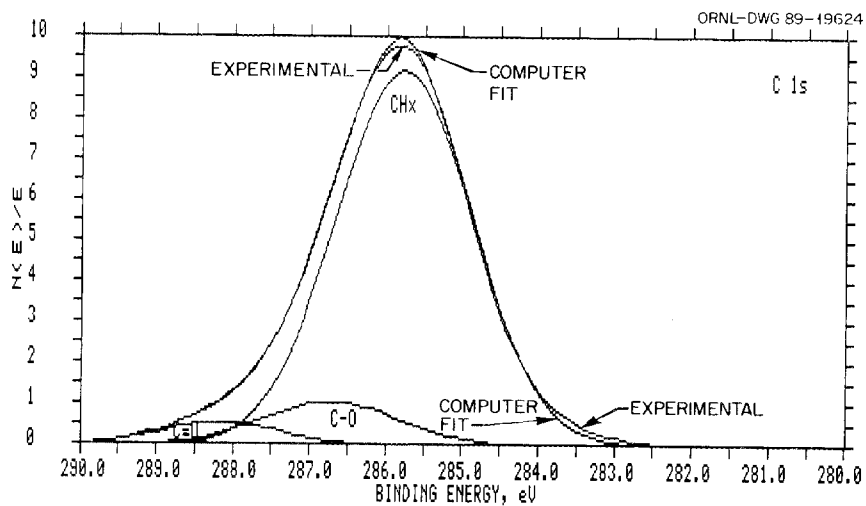


Fig. 20. Computer-fitted electron spectroscopy for chemical analysis spectrum for carbon C1s photoelectron peaks for Blind Canyon coal (A601).

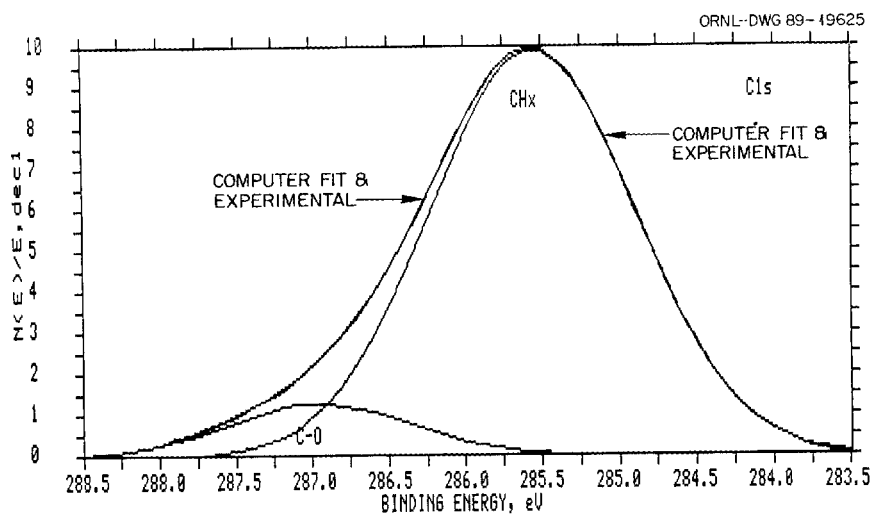


Fig. 21. Computer-fitted electron spectroscopy for chemical analysis spectrum for carbon C1s photoelectron peaks for Pittsburgh #8 coal (A401).

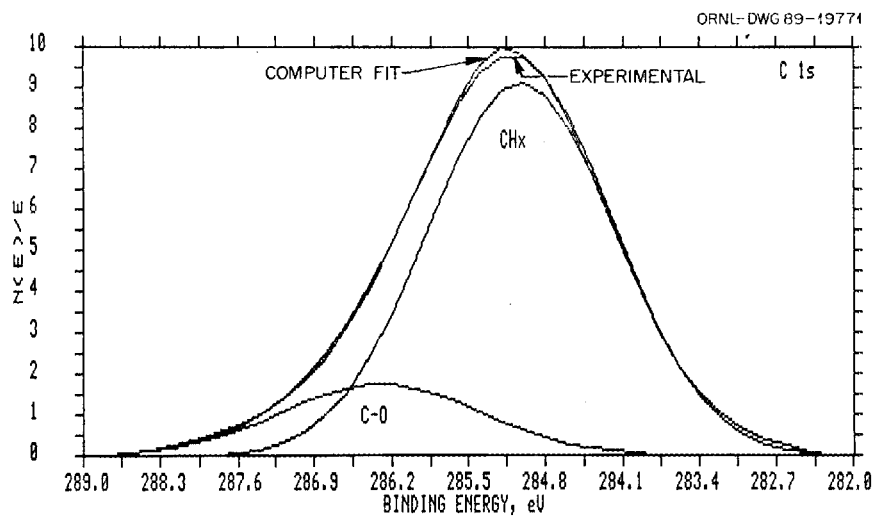


Fig. 22. Computer-fitted electron spectroscopy for chemical analysis spectrum for carbon C1s photoelectron peaks for Upper Freeport coal (A101).

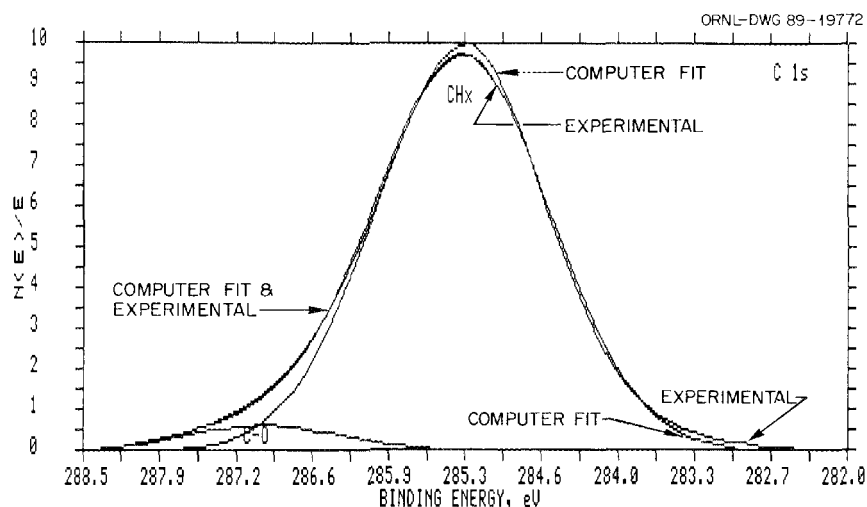


Fig. 23. Computer-fitted electron spectroscopy for chemical analysis spectrum for carbon C1s photoelectron peaks for Pocahontas #3 coal (A501).

computer-aided analyses data from improved instrumentation has led to more information and better quantitative analyses.<sup>9</sup> Few, if any, individual techniques supply as much information related to the chemistry and structure of coals. Recently the use of DRIS has been shown to have considerable merit in the analyses of coals and in situ measurement of the changes wrought in reacting with gaseous reagents.<sup>10,11</sup> Highly regarded researchers in this field have noted that, "Clearly, diffuse reflectance has overwhelming advantages in the characterization of high-ranked coals."<sup>10</sup>

## 5.2 EXPERIMENTAL METHOD

The equipment and techniques for the DRIFT spectroscopic analyses have been described previously.<sup>10-13</sup> The results included here are from a preliminary survey of the ANL coals and all spectra were obtained in a nitrogen purge gas (about 5 ppm moisture) after establishing the equilibrium moisture level. This step required approximately 30 min as demonstrated for spectral levels of moisture that were invariant with time (checked up to 100 h in selected instances). The DRIS optics were of the "on axis" type installed in the standard sample compartment of a Digilab FTS-40 Fourier Transform Spectrometer (FTS). The powdered samples were

used as supplied (-100 mesh) and loosely deposited into the DRIS cup with the sample leveled to the top of the cup with a spatula. Many scans (2000 in this instance) were used to obtain an averaged interferogram prior to Fourier transform (FT) to the frequency domain to obtain spectra with moderately good signal-to-noise ratios.

The spectra were assigned the same code numbers as those given in Table 1 and are presented here as Figs. 24-31 for the corresponding materials. The data are presented in the absorbance format for two reasons. First, the data are similar to classical infrared transmission experiments and hence are functionally simpler to interpret. Second, the use of other methods of presentation (i.e., remission function) are often not warranted when one notes that the conditions of our experiments are not those outlined in the assumptions of the physical optics analyses. As noted in the next section, the semiquantitative values reported here are not appreciably affected by the choice of method for data presentation.

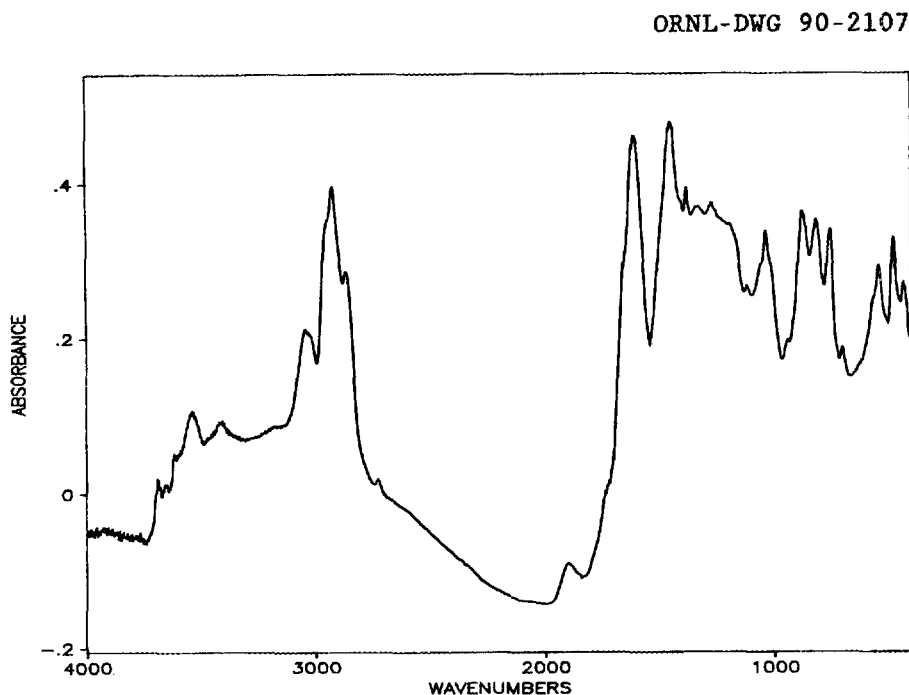


Fig. 24. Diffuse reflectance infrared spectrum of Upper Freeport coal from Pennsylvania.

ORNL-DWG 90-2108

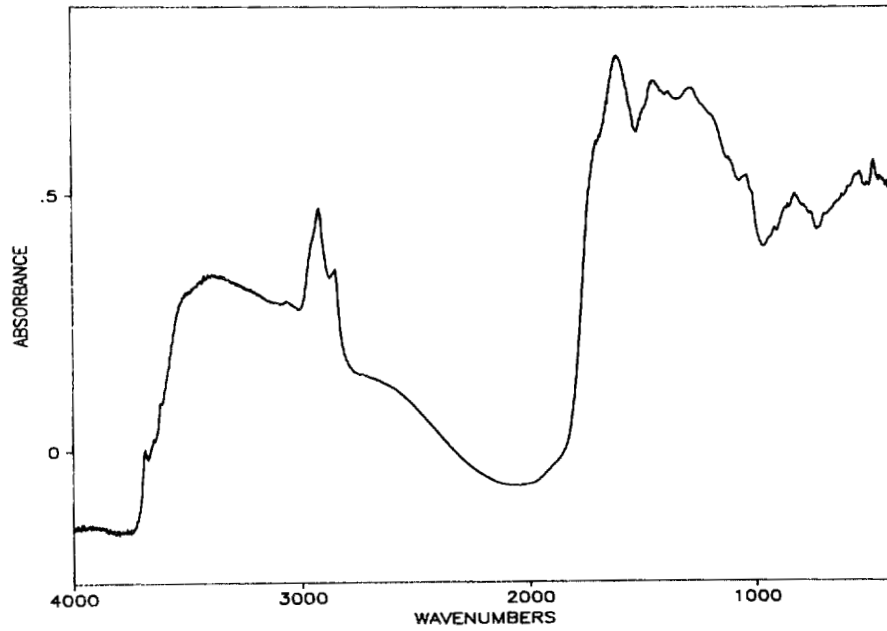


Fig. 25. Diffuse reflectance infrared spectrum of Wyodak coal from Wyoming.

ORNL-DWG 90-2109

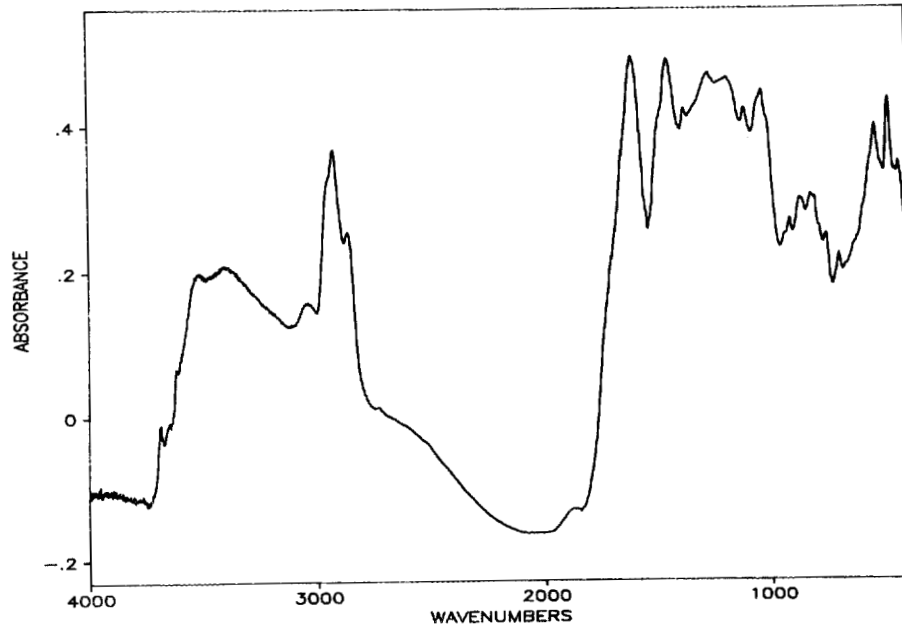


Fig. 26. Diffuse reflectance infrared spectrum of Illinois #6 coal from Illinois.

ORNL-DWG 90-2110

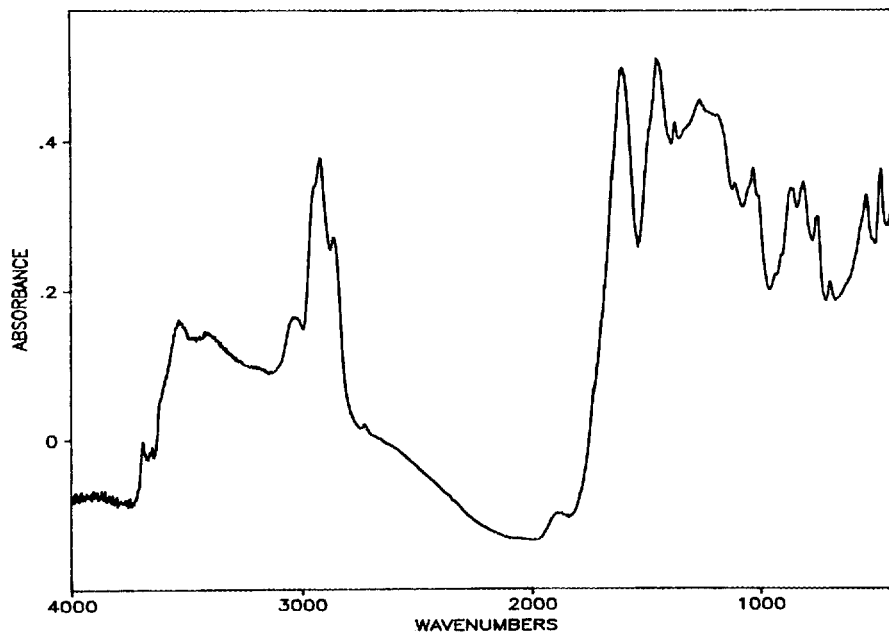


Fig. 27. Diffuse reflectance infrared spectrum of Pittsburgh #8 coal from Pennsylvania.

ORNL-DWG 90-2111

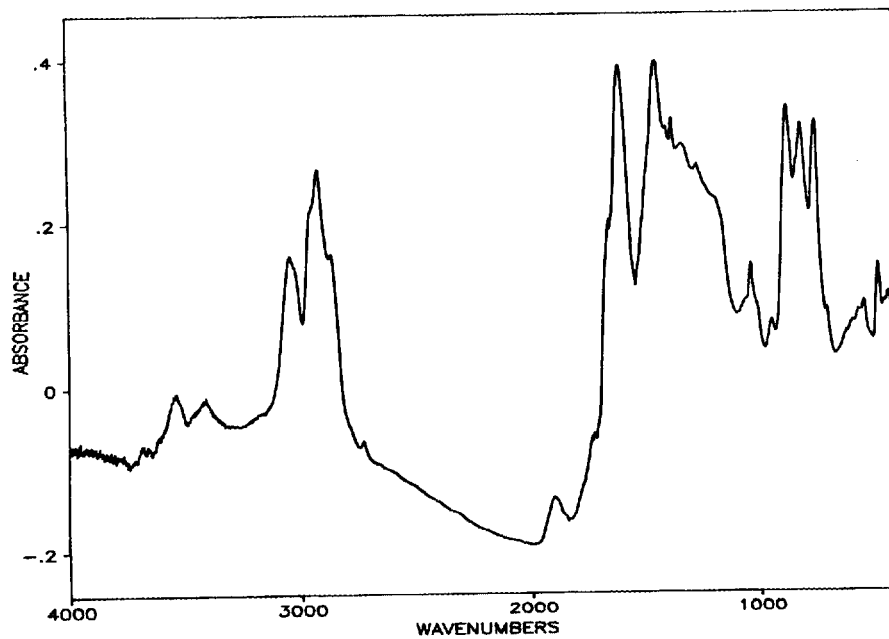


Fig. 28. Diffuse reflectance infrared spectrum of Pocahontas #3 coal from Virginia.

ORNL-DWG 90-2112

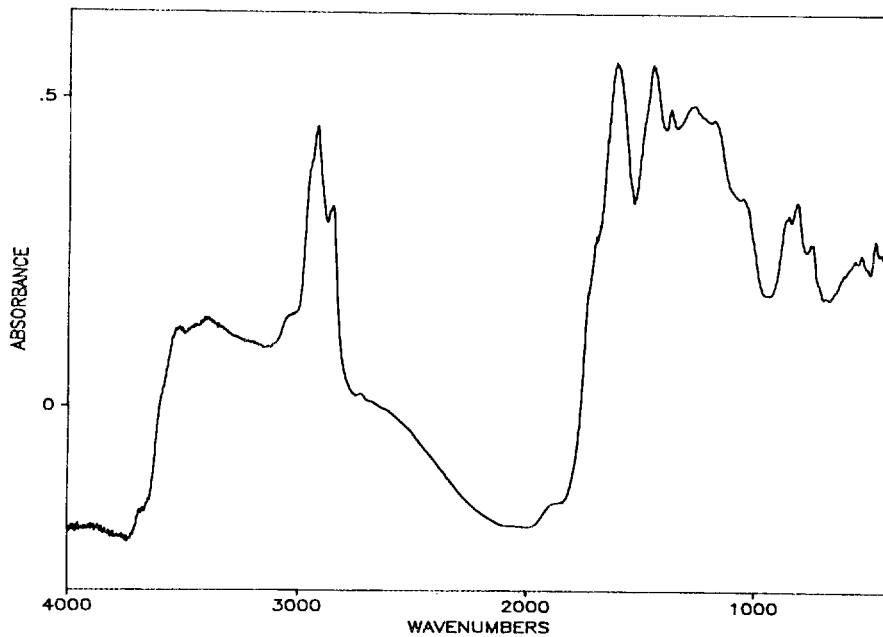


Fig. 29. Diffuse reflectance infrared spectrum of Blind Canyon coal from Utah.

ORNL-DWG 90-2113

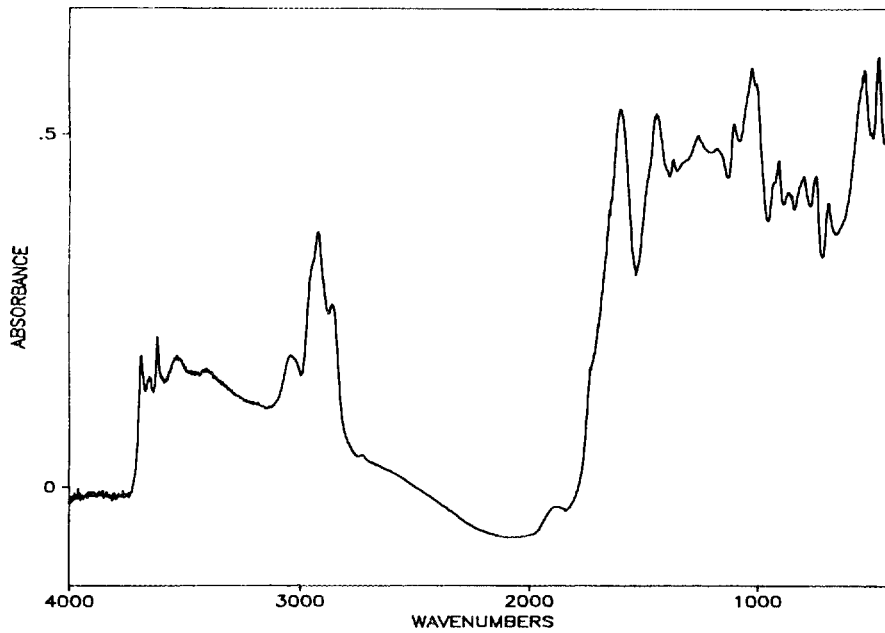


Fig. 30. Diffuse reflectance infrared spectrum of Lewiston-Stockton coal from West Virginia.

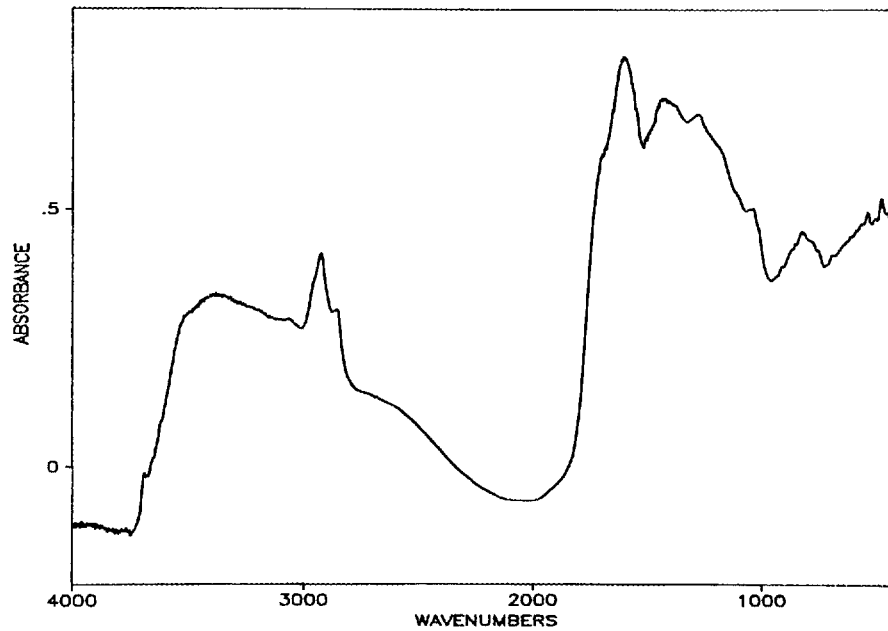


Fig. 31. Diffuse reflectance infrared spectrum of Beulah Zap coal from North Dakota.

### 5.3 RESULTS AND DISCUSSION

Analysis of any one of the accompanying spectra leads to some very important conclusions illustrated in the composite spectrum of Fig. 32. This is a spectrum obtained using equal volumes of each of the described eight coal samples prepared using extensive mixing in a vial and identified as AMIX1. Very prominent features arise from the absorption of energy at specific wavelengths, indicating resonant interactions in the coal structure. Any given spectrum alone can be used only in a qualitative manner to show the presence or absence of specific chemical components. By systematic comparison of various samples, additional information concerning the amounts (relative and/or absolute) of each component can be estimated, and a model for the coal structure can perhaps be constructed. This is a preliminary analysis of the data and will serve to show that the DRIS technique has considerable merit in coal classification in terms of the classical parameters (rank, energy content, chemical composition, proximate analysis, etc.).

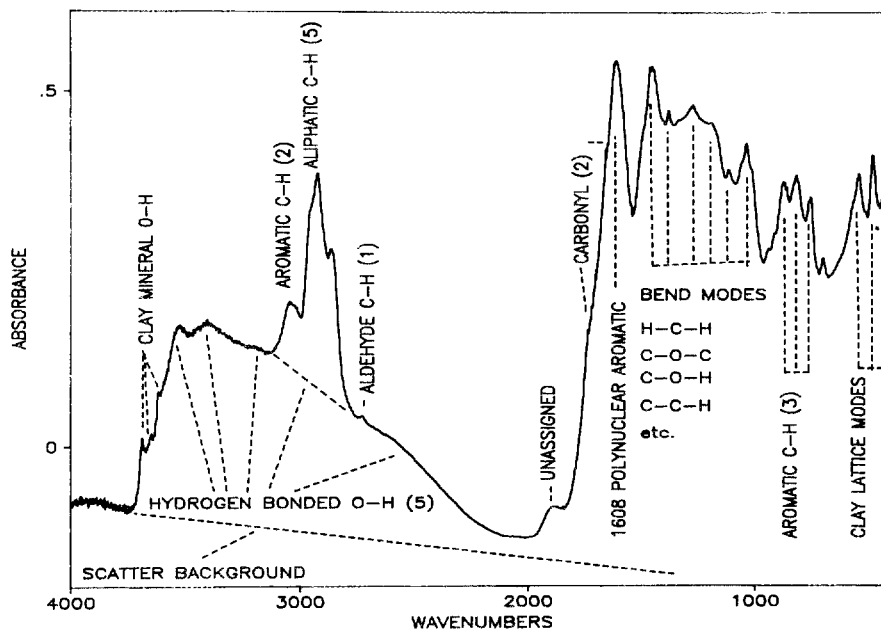


Fig. 32. Diffuse reflectance infrared spectrum of mixed Argonne premium coal samples.

### 5.3.1 Hydrocarbons: Aliphatic and Aromatic

The absorbance peaks ranging from 2800 to 3200 wavenumbers are classically associated with the various C-H vibrational modes. In general, one finds the aromatic species giving rise to the smaller feature above 3000 wavenumbers and the various vibrations of the R-CH<sub>3</sub>, R<sub>2</sub>CH<sub>2</sub>, and R<sub>3</sub>CH entities in aliphatic systems. Interpretation of the multiplet character of these bands is beyond the scope of this work and is not important in the trend analyses reported here. The peak heights above a tangential baseline were used as a measure of the relative number of chromophores present in a given sample. Also note the small peak at about 2740 wavenumbers that is identified with the aldehydic hydrogen (R-CHO). Such a structure is reasonably expected in coals if, as presently thought, virtually all carbon-oxygen functional groups are encountered in the coalification processes. Another interesting feature is the peak that occurs at about 1905 wavenumbers. It has not been satisfactorily assigned as resulting from any specific functionality in the coal structure.

Figure 33 is a graphical presentation of the trends of peak intensities as possible indicators of the coalification processes. The aliphatic peak does not appear to follow any smooth trend with the apparently random scatter as a function of carbon content. In contrast, the aromatic content of the coals increases quite linearly with the increase in carbon content as noted by the open circles of Fig. 33. The 1905 wavenumber band also increases in intensity somewhat linearly as shown in the tenfold scale expansion and the filled squares. Whatever entity is responsible for the light absorption at this frequency, its concentration does serve as a ranking measure for the coals and can consequently be used as a diagnostic measurement indicator. Not too surprisingly, the aldehyde entity (2730 wavenumbers) does not provide a clear trend, but shows a maximum concentration of all doses in the intermediate range of coalification.

### 5.3.2 Aromatic Structures

It is generally recognized now that a more extensive aromatic structure is generated as the coalification process proceeds (at least up

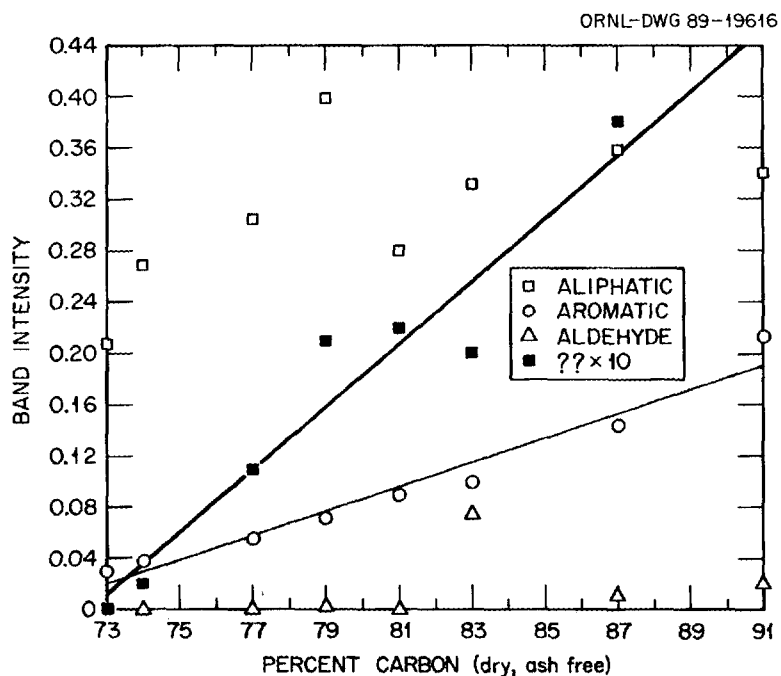


Fig. 33. Diffuse reflectance infrared spectroscopic evaluation of coalification trends.

to the anthracite/graphite end point where dehydrogenation is required) and the near constant 5.5% hydrogen concentration must be reallocated in the process. This aromatizing hydrogenation is quite prominently displayed in the triplex bands at about 850 wavenumbers, as noted in the composite spectrum of Fig. 32. This feature is quite interesting and has been described in detail.<sup>8</sup>

If the total hydrogen content is constant, then the ratio of aromatic to aliphatic species might increase with increase in rank. This indeed is true, as noted by the data of Fig. 34. The polynomial fit (third order) follows the monotonic increase well within the experimental error associated with the round symbols in the figure. This figure shows only a ratio of the line intensities and thus does not include correction for the proper extinction coefficients. However, the observed correlation does appear quite promising. Regardless of the complexities of interpretation and chemical interactions, simplified data processing as discussed here provides an excellent reference curve for ranking of unknown coals. This ratiometric method has merit in that it involves the two peaks of a given sample and should therefore be relatively free of errors in reproducibly

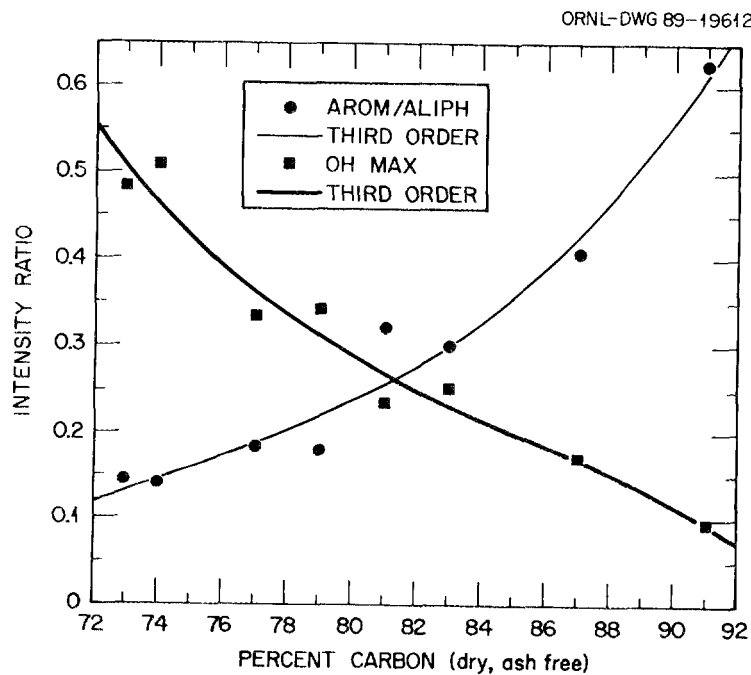


Fig. 34. Diffuse reflectance infrared spectroscopic evaluation of rank dependent properties.

preparing samples. All of the other measurements are absolute intensities and depend somewhat on sample preparation (powder compaction, particle size, sample cup placement, optical alignment, etc.).

### 5.3.3 Hydroxyls: Phenolic, Alcoholic, Acidic, and Aquatic

The large triangular-shaped feature in the AMIX1 spectra of Fig. 32 is due to the resonance with the O-H stretching mode of the various hydroxyl entities in the coal structure. A free isolated O-H stretch is energetically related to a 3740 wavenumber band (narrow, sharp, and distinct). In the crowded environs of the solid coal there are many electron donor species (other O-H, C=O, conjugated  $\pi$  bonds, etc.) that interact to form the classical hydrogen bonds that we schematically represent as O-H...X to denote a nonsigma bond to the X electron donor. The resonant frequencies are shifted to lower wavenumbers as the hydrogen bonding energy increases.

In this work the characteristic maximum intensity was measured above the tangential baseline and used as an indicator for the degree of coalification. These maxima occur near 3600 wavenumbers in contrast to the 3200 wavenumbers used by others.<sup>8</sup> The results are essentially the same except that, due to the geometry of the triangular feature, they have a corresponding lower magnitude of signal. The results in Fig. 34 show the monotonic loss of O-H species at least partially contributing to the gain of aromatic hydrogen as the total inventory of hydrogen remains fixed at the 5.5 wt % over this range of carbon of 72-92%.

These spectra were obtained at very low ambient water vapor concentration in the purge gas of the spectrometer. Thus, all loosely bound molecular water was lost. This situation corresponds to the classical "moisture content" of the coals that is lost at about 100-110°C in air or in vacuo at room temperature.<sup>9</sup> All of the hydroxyls measured in this work, therefore, represent structures tightly held by sigma bonds (phenols, alcohols, acids), minerals (clays, metal hydroxides, etc.), and/or stoichiometric hydrates ( $\text{CaSO}_4 \cdot 2\text{H}_2\text{O}$ ,  $\text{Na}_2\text{SO}_4 \cdot 10\text{H}_2\text{O}$ ,  $\text{NaOH} \cdot \text{H}_2\text{O}$ , etc.). The dry experimental conditions limited the observations to chemically bound species since all physical sorption will be lost at this chemical potential. The bed moisture of these samples can vary from 25-30% for the

lignites to only 1-5% for the higher ranked bituminous coal samples. The DRIFT technique is one of the very few that can analyze this component of coals.<sup>9</sup> Future work will deal with modeling of this poorly understood material.

#### 5.3.4 Minerals

The composite spectrum of Fig. 32 can be used to exemplify the characteristic features associated with the mineral content of the coals. The small sharp peaks located within the coal O-H bands above about 3800 wavenumbers arise from the O-H groups which are located in the clay mineral structures within the coal (kaolinitic, illitic, etc.). The magnitude of these bands can be used to quantitatively measure the individual clay content of each coal.<sup>9</sup> The clay concentration is not readily correlated with the coal rank and is undoubtedly associated with the metamorphic processes occurring in individual coal beds (note high levels in A701/high volatile bituminous coal and low levels in A501/low volatile bituminous coal, with intermediate amounts present in other samples). Clays also give rise to low wavenumber bands due to the lattice vibrational modes in the distinct crystal structures, as pointed out in Fig. 32.

## 6. CONCLUSIONS

Application of several analytical techniques to different types of coal has shown that a combination of electron microscopy, electron spectroscopy, and infrared spectroscopy can provide significant information regarding coal composition and internal structure. The results also indicated that the location and way in which certain elements are bound in the coal can be determined by using a combination of these techniques. Use of electron microscopy allowed direct observation of the structure of minerals and contaminant elements in the coal structure, but was particularly difficult to apply to coals below bituminous in rank. DRIFT can sample a coal surface directly and can provide bonding frequency information, which can often be interpreted with the aid of other information from the literature. Combining these techniques, therefore,

can provide information on the location and concentration of various elements and phases within coal particles. Automation or semiautomation of these techniques could potentially provide powerful correlations between the composition and structure of the bulk coal, ground coal, and the effluents from the combustion process on a large scale. Such a correlation would provide direct information regarding elements and phases, which make the major contributions to undesirable combustion gas effluents.

Future work will focus on applying the microscopy techniques to other coals of bituminous rank followed by comparisons between the new results and those reported here. In addition, ESCA studies will include coals other than those of the ANL suite, but of similar rank, to determine if coals of similar rank have similar contaminant elemental binding energies. The DRIFT technique will be applied to a number of coals during and following grinding to determine if bonding changes can be detected during the comminution process.

## 7. ACKNOWLEDGMENTS

The authors express appreciation to James Hickerson of the Pittsburgh Energy Technology Center for his support in sponsoring this program at ORNL. Special thanks are expressed to A. Choudhury, J. I. Federer, and R. L. Beatty for reviewing the manuscript; D. D. Conger for typing the draft; F. M. Foust for assembling the draft and proofreading; P. H. Miller for editing; and M. R. Upton for final preparation of the report.

## 8. REFERENCES

1. E. L. Fuller, Jr., "Physical and Chemical Structure of Coals: Sorption Studies," in *Coal Structure*, ed. M. L. Gorbaty and K. Ouchi, *Adv. Chem. Ser.* 192, 294 (1981).
2. K. S. Vorres, *Proc. Div. Chem. ACS*, 33 (September 1988), proceedings of symposium, Research on Premium Coal Samples.
3. J. R. Brown, B. I. Kronberg, and W. S. Fyfe, *Fuel* 60, 439 (1981).
4. D. T. Clark and R. Wilson, "ESCA Applied to Aspects of Coal Surface Chemistry," *Fuel* 62, 1034 (1983).

5. D. L. Perry and A. Grint, "Applications of XPS to Coal Characterization," *Fuel* **62**, 1024 (1983).
6. L. W. van Krevelen, *Coal: Typology-Chemistry-Physics Constitution*, Elsevier, 1981, p. 393.
7. P. R. Solomon and R. M. Carangelo, "FTIR Analysis of Coal: 2. Aliphatic and Aromatic Hydrogen Concentration," *Fuel* **67**, 949 (1988).
8. E. L. Fuller, Jr., and N. R. Smyrl, "Chemistry and Structure of Coals: Diffuse Reflectance Infrared Spectroscopy Equipment and Techniques," *Fuel* **64**, 1143 (1985).
9. N. R. Smyrl and E. L. Fuller, Jr., "Diffuse Reflectance Infrared Fourier Transform (DRIFT) Spectroscopic Studies of Coals: In Situ Studies of Acetylation," *Appl. Spectroscopy* **41**, 1023 (1987).
10. P. Painter, B. Bartges, D. Plasizvske, T. Plasizyski, A. Lichtus, and M. Coleman, "Novel Methods for FTIR Analyses of Coal," *J. Am. Chem. Soc.* **31**, 65 (1986).
11. E. L. Fuller, Jr., N. R. Smyrl, and R. L. Howell, "Chemistry and Structure of Fuels: Reaction Monitoring with Diffuse Reflectance Infrared Spectroscopy," in *Chemical, Biological and Industrial Applications of Infrared Spectroscopy*, ed. J. R. Durig, Wiley-Interscience, 1985.
12. N. R. Smyrl and E. L. Fuller, Jr., "Chemistry and Structure of Coals: Diffuse Reflectance Infrared Fourier Transform (DRIFT) Spectroscopy of Air Oxidation," in *Coal and Coal Products: Analytical Characterization Techniques*, ed. E. L. Fuller, Jr., *Am. Chem. Soc. Symp. Ser.* **205**, 133 (1982).
13. N. R. Smyrl, E. L. Fuller, Jr., and G. L. Powell, *Appl. Spectroscopy* **37**, 38 (1983).

## INTERNAL DISTRIBUTION

1-2.	Central Research Library	29-33.	E. L. Fuller, Jr.
3.	Document Reference Section	34-38.	L. A. Harris
4-5.	Laboratory Records Department	39.	E. H. Lee
6.	Laboratory Records, ORNL RC	40.	R. R. Judkins
7.	ORNL Patent Section	41.	J. R. Keiser
8-10.	M&C Records Office	42-46.	T. A. Nolan
11-15.	L. F. Allard	47.	J. O. Stiegler
16.	R. L. Beatty	48-67.	V. J. Tennery
17.	A. Bleier	68.	D. F. Wilson
18.	R. A. Bradley	69.	A. D. Brailsford (Consultant)
19.	D. N. Braski	70.	H. D. Brody (Consultant)
20.	P. T. Carlson	71.	D. P. Pope (Consultant)
21-25.	D. W. Coffey	72.	M. L. Savitz (Consultant)
26.	D. F. Craig	73.	E. R. Thompson (Consultant)
27.	C. S. Daw	74.	J. B. Wachtman (Consultant)
28.	C. H. DuBose		

## EXTERNAL DISTRIBUTION

- 75-86. DEPARTMENT OF ENERGY, Pittsburgh Energy Technology Center,  
P.O. Box 10940, Pittsburgh, PA 15236
- K. Downey (3)  
M. L. Gray  
P. Goldberg  
V. Hathi  
J. D. Hickerson  
M. Keane (4)  
R. W. Lai
- 87-88. DEPARTMENT OF ENERGY, Oak Ridge Operations, P.O. Box 2001, Oak Ridge,  
TN 37831-8600
- E. E. Hoffman  
Office of Assistant Manager for Energy Research and  
Development
89. DEPARTMENT OF ENERGY, Office of Patent Counsel, Chicago Operations  
Office, 9800 South Cass Avenue, Argonne, IL 60439
- 90-99. DEPARTMENT OF ENERGY, Office of Scientific and Technical Information,  
Office of Information Services, P.O. Box 62, Oak Ridge, TN 37831
- For distribution by microfiche as shown in DOE/OSTI-4500,  
Distribution Category UC-102 (Coal Preparation).